Modeling acetylcholine esterase inhibition resulting from exposure to a mixture of atrazine and chlorpyrifos using a physiologically-based kinetic model in fish

Corentin Mit, Cleo Tebby, Tristan Gueganno, Anne Bado-Nilles, Rémy Beaudouin

Modeling acetylcholine esterase inhibition resulting from exposure to a mixture of atrazine and chlorpyrifos using a physiologically-based kinetic model in fish

Corentin Mit [a,b,c], Cleo Tebby [a], Tristan Gueganno [a], Anne Bado-Nilles [b,c],

Rémy Beaudouin [a,b,*]

[a] Unité METO (Modèles pour l'Ecotoxicologie et la Toxicologie), INERIS, 60550 Verneuil en Halatte, France

[b] INERIS, UMR-I 02 SEBIO, Parc ALATA, BP2, 60550 Verneuil-en-Halatte, France

[c] Unité ECOT (Ecotoxicologie in vitro et in vivo), INERIS, Parc ALATA, BP2, 60550 Verneuil-en-Halatte, France

[*] Corresponding author at: Unité METO (Modèles pour l'Ecotoxicologie et la Toxicologie), INERIS, 60550 Verneuil en Halatte, France.

E-mail address:remy.beaudouin@ineris.fr(R. Beaudouin).

Abstract

Aquatic organisms are exposed to mixtures of chemicals that may interact. Mixtures of atrazine (ATR) and chlorpyrifos (CPF) may elicit synergic effects on the permanent inhibition of acetylcholinesterase (AChE) in certain aquatic organisms, causing severe damage. Mechanistic mathematical models of toxicokinetics and toxicodynamics (TD) may be used to better characterize and understand the interactions of these two chemicals. In this study, a previously published generic physiologically-based toxicokinetic (PBTK) model for fish was adapted to ATR and CPF. A sub-model of the kinetics of one of the main metabolites of CPF, chlorpyrifos-oxon (CPF-oxon), was included, as well as a TD model. Inhibition of two esterases, AChE and carboxylesterase, by ATR, CPF and CPF-oxon, was modeled using TD modeling of quantities of total and inactive esterases. Specific attention was given to the parameterization and calibration of the model to accurately predict the concentration and effects observed in the fish using Bayesian inference and published data from fathead minnow (Pimephales promelas), zebrafish (Danio rerio) and common carp (Cyprinus carpio L.). A PBTK-TD for mixtures was used to predict dose-response relationships for comparison with available adult fish data. Synergistic effects of a joint exposure to ATR and CPF could not be demonstrated in adult fish.

Keywords : *PBTK-TD model ; Atrazine ; Chlorpyrifos ; Mixture ; Acetylcholinesterase ; Carboxylesterase*

List of abbreviation

ATR: atrazine

AChE: acetylcholinesterase

CES: carboxylesterase

CYP450: cytochrome P450

PBTK-TD: physiologically based toxicokinetic-toxicodynamic model

CPF: chlorpyrifos

CPF-oxon: chlorpyrifos-oxon

TCP: trichloropyridinole

TK: toxicokinetic

TD: toxicodynamic

1. Introduction

In environmental biomonitoring programs, biomarkers are increasingly proposed as tool to detect early exposure to xenobiotics or physiological effects [1-3]. Among biomarkers, neuromuscular parameters have proven their interest in the study of the effects of contaminants in the environment [4]. The inhibition of those parameters by pesticides may cause severe damage to the organism. In particular, the inhibition of acetylcholinesterase (AChE), which is involved in the regulation of acetylcholine action in neuromuscular junction, is responsible for various effects, *e.g.* the impairment of swimming behavior [5] or the ability to feed, and may lead to the death of the organism [6]. AChE is also one of the most studied biomarkers in fish [7-9]. Other enzymes can also be inhibited by pesticides, such as carboxylesterases (CEs), which may not cause apparent direct toxicity to the organism [6, 10] but may be involved in a detoxification process. CEs can indeed bind to pesticides and thus act as a "sink" by decreasing the amount of effective pesticide [6, 11].

Atrazine (ATR) and chlorpyrifos (CPF) are among the most commonly used pesticides in the world [12]. CPF is an organophosphate (OP) insecticide that is used in both agriculture and in residential settings [13]. CPF affects the neuromuscular junction in target species by inhibiting AChE [14], both directly, as a parent chemical, and indirectly, via one of its metabolites, CPF-oxon. This metabolite is reported to be a stronger inhibitor of AChE and it has been suggested, that the effect of CPF may be mainly due to its metabolite [14-16]. ATR is a herbicide that belongs to the triazine family and inhibits electron transport mechanisms of photosystem II in target

plants [14]. While ATR is not an AChE inhibitor since it cannot interact at the serine residue of the active site, a decrease of AChE activity is measured in fish [17, 18] after exposure to ATR alone. For this reason, and also because of suspicion of endocrine disrupting effects, ATR was banned by the EU in 2003 [19]. 10 years after the ban, ATR was still responsible over 70% of the undrinkable water in particular because some products of atrazine degradation are slow to disappear [20]. However, levels of atrazine dropped significantly in coastal water from more than 150 to 7 ng/L between 1991 and 2010 [21]. As for CPF, the EU prohibited its use by the non-renewal of its marketing authorization in 2020 because of its potential genotoxicity and developmental neurotoxicity [22]. Nevertheless, the mechanisms of low-dose effects of ATR and CPF as single chemicals and in mixture are still unclear.

Aquatic organisms are exposed to multiple chemicals in the aquatic environment. Certain chemicals may interact with each other and cause greater (synergism) or smaller effects (antagonism) than expected based either on the addition of concentrations of the single chemicals [23] or on independent effects [24]. A greater than additive toxicity of ATR and CPF in mixture was shown in invertebrates [14, 16, 17] and was also observed in zebrafish larvae (*Danio rerio)* and fathead minnow juveniles (*Pimephales promelas*)[5, 25]. However, similar studies in adult fish, such as bluegill (*Lepomis macrochirus*), fathead minnow and common carp (*Cyprinus carpio* L.), were not conclusive about the synergistic effect on AChE inhibition [26, 27]. Synergistic effects were suggested to be the result of an increase in synthesis of cytochrome P450 (CYP450) enzymes due to the presence of ATR [28]. This increase would lead to a higher metabolization of CPF into its two metabolites, chlorpyrifos-oxon (CPF-oxon) and trichloropyridinole (TCP) (Figure 1) in carp and zebrafish [26, 27].

Physiologically-based toxicokinetic models (PBTK) are useful tools to improve understanding of the fate of a chemical or a mixture inside an organism [29-31]. Recently, Grech, et al. [32] proposed a generic PBTK model for four different fish, including zebrafish, threespine stickleback (*Gasterosteus aculeatus)*, rainbow trout (*Oncorhynchus mykiss)* and fathead minnow. The construction of a PBTK model with a toxicodynamic (TD) component that predicts effects at the target organs can improve the understanding of toxicity mechanisms, by testing various hypotheses, and be relevant for risk assessment [10, 33, 34]. Moreover, PBTK-TD models for mixtures can help understand mixture effects by quantifying the contribution of kinetics and dynamics to any possible toxicological interactions. Such tools have been applied in rats for several mixtures [33, 35-37]. In fish, only two models have been developed so far [10, 29]. One of them successfully described interaction between melamine and cyanuric acid. It was shown to be mostly due to the chemical interaction at the target organ and demonstrated the usefulness of such models [29].

This paper aims to give new insight on the toxicokinetics and toxicodynamics of ATR and CPF by using both *in silico* methods and experimental data from the literature.

2. Materials and methods

We extended the PBTK model developed by Grech, et al. [32] in order to account for the kinetics of both ATR, CPF, and CPF-oxon, which is the most toxic metabolite of CPF. The toxicodynamic part of the model represented inhibition of AChE and CEs by ATR, CPF and CPF-oxon and was based on the equations previously proposed [10, 33, 34] in rainbow trout and rat. Model parameters were calibrated using experimental data relative to internal kinetics in several fish species and to enzyme inhibition in the common carp. The PBTK-TD model was then adapted to predict effects on esterase inhibition of a mixture of CPF and ATR with the aim of assessing potential induction of CPF metabolism by ATR.

2.1. Experimental data

A full description of the data used can be found in SI section 2.1. TK and TD data obtained *in vivo* in fish exposed to ATR, CPF, or both was collected from the literature in a total of 12 publications (see Table S1 in SI). TD dataset reported *in vivo* AChE and CEs inhibition in a context of exposure to ATR, CPF or mixture of both. Among these studies, Xing, et al. [17] was selected to develop our model, because they provided a complete description of the exposure scenarios as well as a study of both ATR and CPF, and a mixture of both, with the same experimental design. In addition to *in vivo* data, *in vitro* data from the literature was used for the TD sub-model (Table S2 and S3 in SI). The data had been obtained on mice, rat and trout [6, 10, 38, 39].

2.2. Model structure

The PBTK model used is based on the generic model developed by Grech, et al. [32]. This model has been successfully applied to four different species including rainbow trout, zebrafish, fathead minnow and threespine stickleback. The PBTK model was extended to model the kinetics of both CPF and its toxic metabolite, CPF-oxon, and the kinetics of ATR. Absorption was assumed to be branchial due to the lack of information regarding gastro-intestinal absorption of ATR and CPF and because the data on kinetics was obtained using waterborne exposure to ATR of CPF. Excretion was assumed to be mediated by gills, and/or bile. Metabolization was assumed to take place only in liver and was described using a Michaelis-Menten equation (CPF and its metabolites, CPF-oxon and TCP) or first order clearance (ATR) (see Figure S1).

Equations modeling the toxicodynamics of AChE and CEs inhibition were added to the PBTK based on the work of Timchalk and Poet [33] and Abbas and Hayton [10], on rat and trout, respectively, initially developed for organophosphates. Although, AChE inhibition by ATR was probably the result of an indirect interaction between ATR and AChE, the same equation was used to describe this process. In this case, the equation is used as an empirical description of the effects, of ATR on AChE [40]. Indeed, inhibition could occur before AChE protein level, maybe at the ache gene transcriptional level [41].

Synthesis of each enzyme was modeled in brain, muscle, and liver with a zero-order synthesis rate, K_s (nmol.d^{-1}) and a first-order degradation of esterases with K_d (d^{-1}), with organ-specific values. Binding of CPF and CPF-oxon to AChE and CEs was assumed to be irreversible, as reactivation of inhibited AChE was assumed to be insignificant [42].The indirect inactivation of AChE by ATR was assumed to be irreversible as well. Inhibition of both esterases was modeled using a bimolecular inhibition rate constant K_i (nmol^{-1}.d^{-1}) (*Eq. 1*).

$$dQ_{esterase} = K_s \quad - Q_{esterase} \times (K_d + (K_i \quad \times Q_{chemical})) \qquad (1)$$

With $Q_{esterase}$ the quantity of unbound (CPF/ CPF-oxon) or inactivated (ATR) esterase in the tissue (nmol) and $Q_{chemical}$ the quantity of active CPF, CPF-oxon, or ATR in the tissue (nmol).

2.3. Model parameterization

Most of physiological parameters of the model for rainbow trout and fathead minnow had been collected by Grech, et al. [32] (see Table S4 in SI section 2.3). In the present paper, TD processes were modelled with additional physiological parameters, for example, the enzyme levels in tissues. Model performance was increased by calibrating a small number of TK and TD parameters, that were determinant towards whole-body concentrations, using experimental data and Bayesian methods (Monte Carlo Markov Chains, MCMC) (see SI section 2.4). TK and TD parameters were calibrated together since enzyme inactivation by the chemicals affects the kinetics of ATR, CPF, and CPF-oxon**.**

2.3.1. Toxicokinetics

Chemical-specific TK parameters from the literature were obtained from the literature or using QSAR models by Grech, et al. [32] and listed in Table 1 and 2. Parameter values for Michaellis-Menten metabolism (*Km* and *Vmax*) of CPF into CPF-oxon and TCP were obtained *in vitro* [43]. Partition coefficients for CPF and CPF-oxon were estimated using a QSAR method based on *logKow* (CPF-oxon *logKow* =3.5, CPF *logKow* =4.96, according to PubChem) and tissue composition [32, 44] . Kinetics of CPF-oxon metabolism were assumed to be the same as the kinetics of CPF into TCP.

Calibration of the unbound fraction in blood (*UF*) and the blood:water partition coefficient (PC_{BW}) was based on whole-body concentrations resulting from continuous exposure to CPF reported in fathead minnow in two different studies [15, 16], and on the quantity of non-metabolized CPF excreted by the gills which was reported to be approximately 2% of total amount excreted in guppies (*Poecilia reticulata*) [45] (for details see SI section 2.4). Prior distribution of PC_{BW} was based on the QSAR estimate. Tissue:blood partition coefficients were estimated using both a QSAR model and the best fit estimate of PC_{BW}. Since no data on CPF-oxon kinetics was available, including in other species, parameter values for CPF-oxon were not calibrated.

ATR tissue:blood partition coefficients were set to *in vivo* measurements in whitefish (*Coregonus fera*) [46]. In addition, due to the lack of data in fish, the *UF* of ATR in blood was set to 0.74 as reported in rat [47]. We considered an ATR hepatic clearance of 0.024 mL/d/g liver determined in rainbow trout based on the negligible *in vitro* clearance reported by Han, et al. [48]. The blood:water partition coefficient (PC_{BW}), biliary excretion rate (Ke_{bile}) and transfer rate from bile bladder to the gastrointestinal tract lumen (K_{BG}) were calibrated using the PBTK model for zebrafish and whole body concentrations in juvenile zebrafish during exposure and depuration phases (Table S1 in SI) [49]. Prior distributions for K_{BG} and Ke_{bile} were non-informative; PC_{BW} prior distribution was based on the value measured *in vivo* in whitefish (*Coregonus fera)* [46].

2.3.2. Toxicodynamics

The toxicodynamic parameters that regulate the dynamics of AChE and CEs at steady state were either collected from the literature (Table S2 and S3 in SI section 2.2) or calibrated. The enzyme inhibition rates collected from experimental studies and used for calibration were arcsine transformed.

The degradation rate constants (K_d) of AChE in brain, muscle and liver were set to the values estimated using a dose-response modeling approach in rainbow trout [50], i.e. 1.75×10^{-3} d^{-1}, 1.4×10^{-2} d^{-1}, and 1.12×10^{-1} d^{-1} in brain, muscle, and liver respectively. The degradation rate constants of CEs were assumed to be of the same order of magnitude and were therefore set to the same values as AChE, as in the models developed in trout [10, 50] and in rat [34].

Initial quantities of AChE and CEs in brain, muscle and liver were calibrated, as well as the chemical-specific inhibition rates (K_i) of AChE and CEs for ATR, CPF, and CPF-oxon. Calibration was based on *in vivo* inhibition of AChE and CEs activity in muscle and brain measured in dose-response experiments in the common carp (*Cyprinus carpio L.*) exposed to either ATR or CPF [17]. The PBTK model for fathead minnow was used, since both species are Cyprinids. Non-informative prior distributions were used for the *Ki*. Prior distributions of the initial quantities of CEs (nmol/g BW) were based on the values obtained in rats in nmol [51], and transposed to fish by using the relative organ weights in rats, the relative organ weights in fish already used in our PBTK model, and the protein content in rats and fish. Prior distributions of the initial quantities of AChE were in turn estimated assuming that the ratio between AChE and CEs levels was equal to the ratio reported in rats [51] (for details see SI section 2.2).

In order to maintain steady state of enzymes over long periods of simulation time, the synthesis rates (*Ks*) were determined according to Eq. 2 for AChE and CEs in each organ.

$$K_S = Q_{esterase\ initial} \times K_d \qquad (2)$$

2.4. Model applications

A sensitivity analysis of AChE and CEs enzyme inhibition in brain and muscle was performed, according to the exposure scenario used with carps after 40-day exposure and after 20-day depuration [17], and using the variance-based Sobol method [52, 53]. 65 chemical-specific parameters were studied with uniform distributions ±10% of the calibrated parameter values (see SI section 3 for details)

The calibrated PBTK-TD model was used to check how the TD (*i.e.* enzyme inactivation) affected internal concentrations of the xenobiotics. Furthermore, the protective role of CEs was

investigated by predicting AChE inhibition dose-response curves in brain and muscle with and without modeling CEs inhibition.

Mixture effects on AChE and CEs inhibition were predicted without considering induction of CYP450 by ATR, and were compared to dose-response data obtained in the common carp [17] in order to assess the weight of this mechanism. The PBTK-TD model was used to predicted dose-response curves for equitoxic mixtures where each chemical contributes equally to the total toxicity. These dose-response curves were compared to those obtained using the PBTK-TD for single chemicals and Berenbaum's general solution for concentration addition [23].

2.5. Software

Calculations were performed using R version 3.6.1 [54], with packages deSolve [55], sensitivity [56], and GNU MCSim v6.2.0 [57].

3. Results

3.1. Calibration of toxicokinetic and toxicodynamic parameters

Estimates of chemical-specific kinetic and toxicodynamic parameters are reported in Table 2; estimates of initial enzyme quantities are reported in Table 3.

Calibration of ATR parameters mainly improved the elimination kinetics. The estimated PC_{BW} was close to the mode of the prior distribution (prior values in Table S5). Predicted whole-body concentrations in the calibration dataset, obtained in juvenile zebrafish, were relatively accurate: all predictions were within a two-fold factor except for the first uptake timepoint (Figure 2).

The estimate of PC_{BW} for CPF was within a two-fold factor of the QSAR prediction which was used as a prior, with a wide 95% confidence interval ranging from $1.8x10^3$ to $7.91x10^3$. Although the prior distribution was non-informative, the estimate of CPF *UF* (0.0195) was close to the value reported in *Poecilia reticulata* [45]. As presented in the Figure 3, eight out of nine predicted whole-body concentrations were within a 3-fold factor and all were within a 10-fold factor. Predicted CPF concentrations were more accurate for Jarvinen, et al. [15] than Mehler, et al. [16]. The main difference between those two experiments was the longer exposure duration in the first one (Table S1).

The predicted internal concentrations after 40 days continuous exposure to ATR or CPF illustrate the larger bioconcentration factor of CPF: at equal exposure doses: whole body concentrations of CPF were 400-fold greater than ATR concentration levels and 30-fold greater than CPF-oxon (Table S10).

Estimated initial enzyme quantities were mostly close to the prior distributions based on data reported in rat, except for the estimated initial CEs quantity in muscle which was larger than the prior (estimates reported in Table 3 and prior distributions in Table S5)

Bimolecular rate constants (*Ki*) for both AChE and CEs were calibrated with non-informative prior distributions (prior in Table S5, and posterior in Table 2). The estimated bimolecular rate between ACHE and CPF-oxon ($Ki_{AChE/CPF\text{-}oxon}$) was larger than $Ki_{AChE/ATR}$ by two orders of magnitude. The estimated CEs bimolecular rate was the largest for CPF-oxon and was of the same order of magnitude as $Ki_{AChE/CPF\text{-}oxon}$. The estimated $Ki_{CEs/CPF}$ was particularly low. The resulting differences in responses at equivalent internal doses, which take into account the amount of each enzyme in tissues, are illustrated in Figure S13 in SI: inhibition is strongest in muscle, with comparable toxicity of ATR and CPF-oxon.

Comparison of the predicted esterase activity and observations [17] used as a calibration dataset showed that the slope of the predicted dose-responses was systematically too steep (Figure 4). Depuration was particularly badly predicted in brain: predicted activities of both AChE and CEs were almost not affected by the 20-day-depuration whereas observed data showed a clear increase in activity indicating recovery.

3.2. Single chemical model evaluation

The sensitivity analysis (SI section 3) of outputs related to AChE and CEs inhibition showed varying parameter influence depending on the chemical and the enzyme. Interestingly, some TK parameters for ATR, in particular unbound fraction, brain/muscle *PC* and PC_{BW}, were among the ten most influential parameters affecting esterase inhibition (Figure S2 to S5 in SI). Sensitivity analysis also highlighted the importance of CPF-oxon kinetics, including CPF-oxon formation by metabolism of CPF (Michaelis-Menten parameters, *Vmax* and *Km*, Figure S8 and S9) on AChE and CEs inhibition. Among TD parameters, as expected, the bimolecular rates (*Ki*) of a given esterase and a given chemical were often in the three most influential parameters on the esterase inhibition regardless of the exposure, time and organ. However, CEs inhibition in muscle was less influenced by K_i than by K_d of CEs in muscle for ATR and CPF (Figure S5 and S9). The effect of TD on internal concentrations was assessed by also calibrating TK and TD parameters separately (see SI section 4.1 and 4.2). It appears that parameters from TK were the ones mainly affected by the calibration of TK and TD separately (see results of separate calibration in SI section 4.1 and 4.2). In particular, the chemical rate constant from bile to GIT lumen for ATR is much lower when the calibration in done separately (Table S7 in SI). Additional simulations of kinetics with and without the TD part of the model showed that binding to enzymes was responsible for a three-fold decrease in whole body concentrations of CPF-oxon at low doses (up till doses eliciting around 60% AChE activity), an almost two-fold decrease in whole body concentrations of ATR, mostly due to inactivation in muscle, and only around 4% decrease in whole body concentrations of CPF at low doses (see SI section 4.6, Figure S15 in SI). The proportion of active ATR or CPF decreases when exposure doses increase.

Simulations using the PBTK-TD model without modeling binding to CEs illustrates the fact that binding to CEs decreases the amount of available CPF or CPF-oxon by a 10-fold factor in muscle and by a 2-fold factor in brain, therefore contributing to a considerable part in observed toxicity (see SI section 4.7, Figures S16 to S18). Binding to CEs causes a 300-fold decrease in ATR levels in muscle and no significant change in ATR concentrations in brain.

3.3. Model evaluation in mixture

Enzyme inhibition resulting from exposure to the mixtures of ATR and CPF described in Xing, et al. [17] was predicted using the PBTK-TD calibrated for single chemicals and do not account for CPF metabolism induction by ATR. The predictions were close to observations with a maximum discrepancy of 20% between observations and predictions, in particular for the highest dose (Figure 5), but as for the single chemicals, the slope of the dose-response was too steep.

The PBTK-TD model was used to predict dose-response curves for equitoxic mixtures. Doses-response curves were also obtained using the dose-responses predicted using the PBTK-TD for single chemicals and the assumption of concentration addition [23]. The results confirm that the PBTK-TD model for mixtures prediction do not diverge significantly from the dose-responses predicted under the assumption of concentration addition (see Figure S13 in section 4.3 in SI). Minor deviations were observed at high exposure levels in muscle for CEs, and in brain for AChE.

4. Discussion

A PBTK-TD model in fish was successfully developed to predict the uptake and internal kinetics of two pesticides, atrazine and chlorpyrifos, and their impacts on acetylcholinesterase and carboxylesterase inhibition. This model was evaluated by using an external dataset where carps were exposed to mixtures of ATR and CPF. Although the datasets used for calibration were obtained by exposure to single chemicals, the model correctly predicted the observed inhibition caused by exposure to the mixture. Moreover, the dose-response relationship predicted by the PBTK-TD model in fathead minnow was satisfactory, although the concentration addition model used was the most parsimonious; synergistic effects of a joint exposure to ATR and CPF were not demonstrated.

Physiologically based toxicokinetic models coupled to a toxicodynamic model are still scarce in ecotoxicology. In particular, for fish, only three models have been developed so far, two in rainbow trout [10, 29] and one on farmed tilapia *(Oreochromis mossambicus*) [58]. Two of these studies modeled effects of single chemicals, paraoxon and arsenic, whereas Tebby, et al. [29] simulated an exposure to a mixture of melamine and cyanuric acid. Because they are based on the physiology, PBTK models are interesting tools for taking into account interspecies variability. Various datasets describing toxicokinetics are available on species that were not included in the generic model in the first place, such as carp or medaka (*Oryzias latipes*). As shown in the present paper, certain species can be assumed to be similar, or else species-specific parameters can be modified to adapt the model to extra species.

Although they are still rare, the benefit of such PBTK-TD models in mixture is twofold: being able to propose more realistic exposure scenarios since aquatic organisms face multiple, time-dependent exposures, and also being able to link internal concentrations in organs to various effects. Currently, environmental risk assessment promotes a different, more generic approach based on an empirical model, GUTS (General Unified Threshold model) [59]. Though this approach is promising by gathering under the same framework several TK-TD models, they are empirical models and fail to explain the mechanism of action of toxic: effects are only predicted on high-level functions, mainly survival. PBTK-TD models offer the possibility to explain the mechanism of action of toxicants by modeling their effects at target organ. For this reason, they represent a promising development in the future of qAOPs (quantitative adverse outcome pathway) [60].

However, the requirements in experimental data while building such models are rarely met notably because experimental designs rarely consider both TK and TD. In addition, physiological data in fish are usually scarce and sometimes unreliable. For example, in our case, absorption was only considered through the gills whereas it maybe also occurs through

the GIT. Likewise, complex phenomenon, such as blood-brain barrier, which would require a lot of data to be implemented in the generic model are not included although they could improve its predictive capability, notably in the brain. However, in the case of exposure to ATR and/or CPF, the availability of data in several species at different doses and at different organizational levels facilitated the construction of the first PBTK-TD model. Nonetheless, in general, experimental data does not include both variation on dose and time-course, which is a strong limitation for the domain of applicability.

A generic model developed by Grech, et al. [32] was used to predict the TK of ATR, CPF and CPF-oxon, a metabolite of CPF. Physiological parameters of the PBTK model, such as relative blood flows to organs, relative organ volumes, and tissue composition, were set to values as species-specific as possible. The chemical-specific parameterization in the model by Grech, et al. [32] was refined by fitting the model to the observations obtained in two fish species (zebrafish and fathead minnow) in three experimental studies [15, 16, 49]. Although TK observations consisted in whole-body concentrations, the final predictions of esterase inhibition in specific organs were satisfactory, indicating that predicted internal concentrations in organs may be accurate, or at least compensated by the values of the organ-specific TD parameters (initial enzyme quantities). However, using different fish species in the calibration may limit the generalization of the calibrated parameters and be a source of uncertainty. For example, ATR TK parameters were calibrated on a dataset on juvenile zebrafish and may only be valid at this developmental stage. Moreover, the scarcity of the studies on the mixture of ATR and CPF lead us to use a dataset obtained in carps, which was not one of the four model species in the generic PBTK. As common carp and fathead minnow were both Cyprinids, we decided to use fathead minnow model. We assumed that though carps were larger than fathead minnows, their physiological parameters were similar, *e.g.* relative blood flows to organs or the relative weight of organs. Nonetheless, strong variations in metabolism can be expected, as illustrated by the difference in metabolism of CPF into CPF-oxon between two salmonids [43].

Chemical-specific parameters of CPF-oxon were not calibrated due to lack of experimental data. CPF-oxon is generally not detected in tissues [61] because of rapid hydrolysis to TCP [62], as suggested by *in vitro* microsomal biotransformation rates in mouse [63]. Consequently, partition coefficients were estimated using the QSAR method [32] and metabolism for CPF-oxon was chosen to follow the same kinetics as CPF into TCP. Although CPF metabolism has been quantified *in vitro* in trout hepatocytes, metabolism of CPF-oxon has not been quantified. The high sensitivity of the esterase inhibition to CPF and CPF-oxon metabolism rates revealed by the sensitivity analysis underlines that metabolism is an important source of uncertainty in our TK predictions, and could be reduced by producing new experimental data. Overall, predicted

kinetics of both parent chemicals using a small number of calibrated parameters were satisfactory, since most were within a 3-fold factor.

The TD part of this model is based on the first PBTK-TD model in fish [10]. This study modeled the inhibition of CEs and AChE in rainbow trout in presence of paraoxon, an organophosphate related to CPF. However, contrary to Abbas and Hayton [10] who focused on time-courses of paraoxon internal concentrations and effects, TK and TD in our model were predicted and compared to observations at several doses but at only one or two timepoints in each study.

Although the same model structure for AChE inhibition can be used for several species, the TD parameter values may vary considerably from one species to another. Bimolecular inhibition rates are also highly dependent on the species. A 3-fold variation in *Ki* for methyl-paraoxon with AChE was reported in the same study in three fish species [64] where the reaction was assumed to be reversible. In our model, as in other PBTK-TD models for AChE inhibition developed in trout and rodents, the *Ki* were assumed to be independent of substrate concentration. This may be a limitation of the model, since in mice, the efficiency of phosphorylation appeared to decrease with increasing substrate concentration [65].

Enzyme synthesis, degradation rates and concentrations in organs are clearly not sufficiently documented to provide species-specific TD models for AChE in fish. Most of the data reported on AChE inhibition is reported as percent inhibition compared to control, or in the best case as nanomoles of substrate hydrolysed per unit time and weight [11, 66-69]. Consequently, a 15-fold variation in brain and plasma AChE activity per tissue weight has been reported across 16 species [70]. Moreover, variability in AChE activity has even been observed between fish of the same species maintained either in laboratory or *in situ* [66]. The strong interspecies variability in AChE activity may add up to variability in synthesis, degradation and inhibition rates and is likely to result in large differences between species.

Though the data from *in vitro* experimentations helps understand differences in toxicity between chemicals or between species, it could not be directly integrated into our model to predict *in vivo* inhibition due to the fact that many intra-cellular mechanisms were not modeled and do not occur in *in vitro* cell-free experimentations. For example, modeling the dynamics of ButyrylCholinEsterase (BuChE) binding processes during detoxification [6] could increase model realism and performance. This non-target B-esterase binds stoichiometrically with organophosphates explaining their inclusion in a PBTK-TD model of brain AChE inhibition in rat [38, 71]. Although BuChE has been detected in the plasma of some Cyprinid species, it has not been detected in many other fish [70, 72]. The lack of knowledge regarding BuChE compared

to AChE in fish hinders integration of BuChE inhibition in a PBTK-TD model: BuChE tissue levels, synthesis, and degradation rates are unknown.

In our study, inhibition was modelled in the main target organs, brain and muscle, and also in liver. Indeed, the liver was thought to be a large reservoir of CEs and act as a buffer compartment through binding of CEs to metabolites [6, 10]. In Abbas and Hayton [10], the toxicodynamics were described in heart, brain and liver. In addition, other compartments were identified as the place of esterase inhibition such as plasma or muscle in general [6]. Data was too scarce to be able to include plasma esterase levels in our model even though plasmatic CEs may play an important role. For example, in rainbow trout, plasmatic CEs represents as much as 58% of total body CEs activity in adult rainbow trout [68]. Furthermore, as plasmatic CEs is distributed round the body, it may contribute more to detoxifying than liver CEs.

One other limit of the realism and performance of this model was the lack of specific synthesis rate values for CEs, as Abbas and Hayton [10] only proposed *in vivo* synthesis rate values for AChE. In addition, these zero-order synthesis rates imply that synthesis is independent of the actual quantity of enzyme. However, recent studies in adult red crucian carp (*Carassius auratus*) observed an increase of AChE levels after 6 days of exposure to fluoxetine and a backup to normal value after 6 days of recovery [73]. The lack of feedback loop in the model that would modulate AChE synthesis rate could explain the fact that the predicted dose-response relationships (SI section 4.3) were systematically too steep. This may reveal a shortcoming of the model since even increasing 100-fold the degradation constant rates (and thereon increasing also 100-fold the synthesis rate) did not produce satisfactory dose-response slopes.

MCMC calibration on *in vivo* data allowed us to propose bimolecular rate constants of the binding between AChE or CEs and ATR, CPF or CPF-oxon. As highlighted in Coban, et al. [74], differences in experimental protocols resulted in a large variability in *Ki* determined *in vitro*. Thus, Bayesian calibration could provide closer estimates of the biological value of those inhibition rates. The calibrated *Ki* values were largest and of the same order of magnitude for CPF-oxon and ATR: $Ki_{AChE/CPF\text{-}oxon}$ was 2-fold higher than $Ki_{AChE/ATR}$ and three orders of magnitude higher than $Ki_{AChE/CPF}$ and $Ki_{CEs/CPF}$. Our calibrated value for $Ki_{AChE/CPF\text{-}oxon}$, 35.4 $nmol^{-1}.min^{-1}$, was far greater than the value reported for paraoxon, 1.06 $\times 10^{-3}$ $nmol^{-1}.min^{-1}$ [10]. According to the predicted internal concentrations in muscle resulting from 40 days exposure (Table S9 in SI) internal CPF levels are greater than CPF-oxon levels and two to three orders of magnitude higher than ATR levels. CPF has been suggested to be responsible for a large part of AChE inhibition although CPF-oxon is a stronger inhibitor [16, 62, 75]. Given the ratio of predicted internal concentrations and the potency of each chemical regarding enzyme

inhibition (Figure S14 in SI, section 4.5), our findings suggest that CPF-oxon is responsible for more AChE inhibition than CPF. In addition, CPF-oxon may be particularly responsible for the depletion of CEs. ATR has been reported to be responsible for a weak inactivation of AChE [14, 16]. But according to our model predictions, at equal internal concentrations, ATR may be as potent as CPF-oxon. The difference in sensitivity of AChE activity *in vivo* to ATR and CPF therefore appears to be due to the difference in internal concentrations. The strong potency of ATR was unexpected because inactivation of AChE may be the result of indirect toxicity *in vivo* as ATR is not an AChE inhibitor.

In this paper, the PBTK-TD model was built as a tool to investigate the effect of a mixture ATR-CPF on AChE and CEs inhibition. As AChE inhibition plays an important role in neuromuscular junctions and cholinergic synapses, AChE inhibition is a relevant biomarker of exposure [8, 72]. As a detoxifying enzyme, CEs would play a role of protection by binding to pesticides and act as a stoichiometric buffer [10, 17, 72]. Calibrating the PBTK-TD model and the sensitivity analysis showed that the quantities of enzyme alone did not have a decisive role in the TD of esterase inhibition. Rather, the rate of renewal of the enzymes may play a larger role both in the EC50 of the toxic response and in the slope of the dose-response. The data available in carp provided dose-response relationships but information about the time-course of esterase inhibition is lacking. Chemical-independent data on enzyme renewal rates under control conditions would also greatly help to develop TD models.

Although an effect of ATR on CPF metabolism had been envisioned, interactions between ATR and CPF were finally not included in the model since they did not seem necessary. The mixture that had been tested in carp was equimassic, although ATR was roughly one order of magnitude less potent than CPF regarding AChE inhibition. Interactions would be more readily identifiable in an equitoxic mixture since interactions are unlikely to appear in an equimassic mixture of dissimilarly acting chemicals [76]. Nonetheless, because the actions of inhibition by the chemicals were affecting the same pool of esterases, it would have highlighted, if any, an interaction in mixture. It is the advantage of our model to include mechanisms of effects that can interact.

Our mechanistic model predicts AChE inhibition levels equivalent, at least at low doses, to the predictions based on dose-response modeling and concentration addition of external concentrations. This mechanistic model is able to predict sigmoidal dose-response relationships without use of an empirical dose-response function, with differences in shapes that reflect differences in esterase levels in tissues, renewal rates, and inactivation of two different esterases.

Supporting information

Supporting Figure S1-S18 and Supporting Table S1-S10.

References

1. Le Guernic, A.; Sanchez, W.; Palluel, O.; Bado-Nilles, A.; Turies, C.; Chadili, E.; Cavalié, I.; Adam-Guillermin, C.; Porcher, J.-M.; Geffard, A.; Betoulle, S.; Gagnaire, B., In situ experiments to assess effects of constraints linked to caging on ecotoxicity biomarkers of the three-spined stickleback (Gasterosteus aculeatus L.). *Fish Physiology and Biochemistry* **2016,** *42*, (2), 643-657.
2. Sturm, A.; da Silva de Assis, H. C.; Hansen, P. D., Cholinesterases of marine teleost fish: enzymological characterization and potential use in the monitoring of neurotoxic contamination. *Marine Environmental Research* **1999,** *47*, (4), 389-398.
3. Sanchez, W.; Aït-Aïssa, S.; Palluel, O.; Ditche, J.-M.; Porcher, J.-M., Preliminary investigation of multi-biomarker responses in three-spined stickleback (Gasterosteus aculeatus L.) sampled in contaminated streams. *Ecotoxicology* **2007,** *16*, (2), 279-287.
4. van der Oost, R.; Beyer, J.; Vermeulen, N. P. E., Fish bioaccumulation and biomarkers in environmental risk assessment: a review. *Environ. Toxicol. Pharmacol.* **2003,** *13*, (2), 57-149.
5. Perez, J.; Domingues, I.; Monteiro, M.; Soares, A.; Loureiro, S., Synergistic effects caused by atrazine and terbuthylazine on chlorpyrifos toxicity to early-life stages of the zebrafish Danio rerio. *Environmental Science and Pollution Research* **2013,** *20*, (7), 4671-4680.
6. Maxwell, D. M., The specificity of carboxylesterase protection against the toxicity of organophosphorus compounds. *Toxicology and Applied Pharmacology* **1992,** *114*, (2), 306-312.
7. Sarkar, A.; Ray, D.; Shrivastava, A. N.; Sarker, S., Molecular Biomarkers: Their significance and application in marine pollution monitoring. *Ecotoxicology* **2006,** *15*, (4), 333-340.
8. Fulton, M. H.; Key, P. B., Acetylcholinesterase inhibition in estuarine fish and invertebrates as an indicator of organophosphorus insecticide exposure and effects. *Environmental Toxicology and Chemistry* **2001,** *20*, (1), 37-45.
9. Cajaraville, M. P.; Bebianno, M. J.; Blasco, J.; Porte, C.; Sarasquete, C.; Viarengo, A., The use of biomarkers to assess the impact of pollution in coastal environments of the Iberian Peninsula: a practical approach. *Sci. Total Environ.* **2000,** *247*, (2), 295-311.
10. Abbas, R.; Hayton, W. L., A physiologically based pharmacokinetic and pharmacodynamic model for paraoxon in rainbow trout. *Toxicology and Applied Pharmacology* **1997,** *145*, (1), 192-201.
11. Wheelock, C. E.; Eder, K. J.; Werner, I.; Huang, H. Z.; Jones, P. D.; Brammell, B. F.; Elskus, A. A.; Hammock, B. D., Individual variability in esterase activity and CYP1A levels in Chinook salmon (Oncorhynchus tshawyacha) exposed to esfenvalerate and chlorpyrifos. *Aquatic Toxicology* **2005,** *74*, (2), 172-192.
12. Fu, Y.; Li, M.; Liu, C.; Qu, J. P.; Zhu, W. J.; Xing, H. J.; Xu, S. W.; Li, S., Effect of atrazine and chlorpyrifos exposure on cytochrome P450 contents and enzyme activities in common carp gills. *Ecotoxicology and Environmental Safety* **2013,** *94*, 28-36.
13. Ali, D.; Nagpure, N. S.; Kumar, S.; Kumar, R.; Kushwaha, B.; Lakra, W. S., Assessment of genotoxic and mutagenic effects of chlorpyrifos in freshwater fish Channa punctatus (Bloch) using micronucleus assay and alkaline single-cell gel electrophoresis. *Food and Chemical Toxicology* **2009,** *47*, (3), 650-656.
14. Wacksman, M. N.; Maul, J. D.; Lydy, M. J., Impact of atrazine on chlorpyrifos toxicity in four aquatic vertebrates. *Archives of Environmental Contamination and Toxicology* **2006,** *51*, (4), 681-689.
15. Jarvinen, A. W.; Nordling, B. R.; Henry, M. E., Chronic toxicity of dursban (chlorpyrifos) to the fathead minnow (*Pimephales-promelas*) and the resultant acetylcholinesterase inhibition. *Ecotoxicology and Environmental Safety* **1983,** *7*, (4), 423-434.
16. Mehler, W. T.; Schuler, L. J.; Lydy, M. J., Examining the joint toxicity of chlorpyrifos and atrazine in the aquatic species: *Lepomis macrochirus*, *Pimephales promelas* and *Chironomus tentans*. *Environmental Pollution* **2008,** *152*, (1), 217-224.

17. Xing, H. J.; Wang, J. T.; Li, J. L.; Fan, Z. T.; Wang, M.; Xu, S. W., Effects of atrazine and chlorpyrifos on acetylcholinesterase and Carboxylesterase in brain and muscle of common carp. *Environ. Toxicol. Pharmacol.* **2010,** *30*, (1), 26-30.
18. Schmidel, A. J.; Assmann, K. L.; Werlang, C. C.; Bertoncello, K. T.; Francescon, F.; Rambo, C. L.; Beltrame, G. M.; Calegari, D.; Batista, C. B.; Blaser, R. E.; Roman Júnior, W. A.; Conterato, G. M. M.; Piato, A. L.; Zanatta, L.; Magro, J. D.; Rosemberg, D. B., Subchronic atrazine exposure changes defensive behaviour profile and disrupts brain acetylcholinesterase activity of zebrafish. *Neurotoxicology and Teratology* **2014,** *44*, 62-69.
19. Bethsass, J.; Colangelo, A., European Union Bans Atrazine, While the United States Negotiates Continued Use. *International Journal of Occupational and Environmental Health* **2006,** *12*, (3), 260-267.
20. Health, M. o. S. A. a., Bilan de la qualite de l'eau au robinet du consommateurvis-a-vis des pesticides en 2014. In 2016.
21. Nödler, K.; Licha, T.; Voutsa, D., Twenty years later – Atrazine concentrations in selected coastal waters of the Mediterranean and the Baltic Sea. *Marine Pollution Bulletin* **2013,** *70*, (1), 112-118.
22. EFSA, Statement on the available outcomes of the human health assessment in the context of the pesticides peer review of the active substance chlorpyrifos. *EFSA Journal* **2019,** *17*, (8), e05809.
23. Berenbaum, M. C., The expected effect of a combination of agents: the general solution. *Journal of Theoretical Biology* **1985,** *114*, (3), 413-431.
24. Bliss, C. I., The toxicity of poisons applied jointly. *Annals of Applied Biology* **1939,** *26*, (3), 585-615.
25. Tyler Mehler, W.; Schuler, L. J.; Lydy, M. J., Examining the joint toxicity of chlorpyrifos and atrazine in the aquatic species: Lepomis macrochirus, Pimephales promelas and Chironomus tentans. *Environmental Pollution* **2008,** *152*, (1), 217-224.
26. Xing, H. J.; Zhang, Z. W.; Yao, H. D.; Liu, T.; Wang, L. L.; Xu, S. W.; Li, S., Effects of atrazine and chlorpyrifos on cytochrome P450 in common carp liver. *Chemosphere* **2014,** *104*, 244-250.
27. Dong, X.; Zhu, L.; Wang, J.; Wang, J.; Xie, H.; Hou, X.; Jia, W., Effects of atrazine on cytochrome P450 enzymes of zebrafish (Danio rerio). *Chemosphere* **2009,** *77*, (3), 404-412.
28. Jin-Clark, Y.; Lydy, M. J.; Zhu, K. Y., Effects of atrazine and cyanazine on chlorpyrifos toxicity in Chironomus tentans (Diptera : Chironomidae). *Environmental Toxicology and Chemistry* **2002,** *21*, (3), 598-603.
29. Tebby, C.; Brochot, C.; Dorne, J. L.; Beaudouin, R., Investigating the interaction between melamine and cyanuric acid using a Physiologically-Based Toxicokinetic model in rainbow trout. *Toxicology and Applied Pharmacology* **2019,** *370*, 184-195.
30. Gerlowski, L. E.; Jain, R. K., Physiologically based pharmacokinetic modeling: Principles and applications. *Journal of Pharmaceutical Sciences* **1983,** *72*, (10), 1103-1127.
31. Grech, A.; Brochot, C.; Dorne, J.-L.; Quignot, N.; Bois, F. Y.; Beaudouin, R., Toxicokinetic models and related tools in environmental risk assessment of chemicals. *Sci. Total Environ.* **2017,** *578*, 1-15.
32. Grech, A.; Tebby, C.; Brochot, C.; Bois, F. Y.; Bado-Nilles, A.; Dorne, J. L.; Quignot, N.; Beaudouin, R., Generic physiologically-based toxicokinetic modelling for fish: Integration of environmental factors and species variability. *Sci. Total Environ.* **2019,** *651*, 516-531.
33. Timchalk, C.; Poet, T. S., Development of a physiologically based pharmacokinetic and pharmacodynamic model to determine dosimetry and cholinesterase inhibition for a binary mixture of chlorpyrifos and diazinon in the rat. *Neurotoxicology* **2008,** *29*, (3), 428-443.
34. Gearhart, J. M.; Jepson, G. W.; Clewell, H. J.; Andersen, M. E.; Conolly, R. B., Physiologically based pharmacokinetic and pharmacodynamic model for the inhibition of acetylcholinesterase by diisopropyfluorophosphate. *Toxicology and Applied Pharmacology* **1990,** *106*, (2), 295-310.
35. El-Masri, H. A.; Thomas, R. S.; Sabados, G. R.; Phillips, J. K.; Constan, A. A.; Benjamin, S. A.; Andersen, M. E.; Mehendale, H. M.; Yang, R. S. H., Physiologically based pharmacokinetic/pharmacodynamic modeling of the toxicologic interaction between carbon tetrachloride and kepone. *Archives of Toxicology* **1996,** *70*, (11), 704-713.

36. El-Masri, H. A.; Constan, A. A.; Ramsdell, H. S.; Yang, R. S. H., Physiologically based pharmacodynamic modeling of an interaction threshold between trichloroethylene and 1,1-dichloroethylene in fischer 344 rats. *Toxicology and Applied Pharmacology* **1996,** *141*, (1), 124-132.
37. El-Masri, H. A.; Mumtaz, M. M.; Yushak, M. L., Application of physiologically-based pharmacokinetic modeling to investigate the toxicological interaction between chlorpyrifos and parathion in the rat. *Environ. Toxicol. Pharmacol.* **2004,** *16*, (1-2), 57-71.
38. Timchalk, C.; Nolan, R. J.; Mendrala, A. L.; Dittenber, D. A.; Brzak, K. A.; Mattsson, J. L., A Physiologically Based Pharmacokinetic and Pharmacodynamic (PBPK/PD) Model for the Organophosphate Insecticide Chlorpyrifos in Rats and Humans. *Toxicological Sciences* **2002,** *66*, (1), 34-53.
39. Johnson, J. A.; Wallace, K. B., Species-related differences in the inhibition of brain acetylcholinesterase by paraoxon and malaoxon. *Toxicology and Applied Pharmacology* **1987,** *88*, (2), 234-241.
40. Brodeur, J. C.; Poletta, G. L.; Simoniello, M. F.; Carriquiriborde, P.; Cristos, D. S.; Pautasso, N.; Paravani, E.; Poliserpi, M. B.; D'Andrea, M. F.; Gonzalez, P. V.; Aca, V. L.; Curto, A. E., The problem with implementing fish farms in agricultural regions: A trial in a pampean pond highlights potential risks to both human and fish health. *Chemosphere* **2021,** *262*, 128408.
41. Wang, H.; Mu, S. M.; Zhang, F. J.; Wang, H. L.; Liu, H.; Zhang, H.; Kang, X. J., Effects of Atrazine on the Development of Neural System of Zebrafish, Danio rerio. *Biomed Res. Int.* **2015,** *2015*, 10.
42. Wallace, K. B.; Herzberg, U., Reactivation and aging of phosphorylated brain acetylcholinesterase from fish and rodents. *Toxicology and Applied Pharmacology* **1988,** *92*, (2), 307-314.
43. Lavado, R.; Schlenk, D., Microsomal biotransformation of chlorpyrifos, parathion and fenthion in rainbow trout (Oncorhynchus mykiss) and coho salmon (Oncorhynchus kisutch): Mechanistic insights into interspecific differences in toxicity. *Aquatic Toxicology* **2011,** *101*, (1), 57-63.
44. Pery, A. R. R.; Devillers, J.; Brochot, C.; Mombelli, E.; Palluel, O.; Piccini, B.; Brion, F.; Beaudouin, R., A Physiologically Based Toxicokinetic Model for the Zebrafish Danio rerio. *Environmental Science & Technology* **2014,** *48*, (1), 781-790.
45. Welling, W.; de Vries, J. W., Bioconcentration kinetics of the organophosphorus insecticide chlorpyrifos in guppies (Poecilia reticulata). *Ecotoxicology and Environmental Safety* **1992,** *23*, (1), 64-75.
46. Gunkel, G.; Streit, B., Mechanisms of bioaccumulation of a herbicide (atrazine, s-triazine) in a fresh-water mollusk (*Ancylus-fluviatilis Mull*) and a fish (*Coregonus-fera Jurine*). *Water Research* **1980,** *14*, (11), 1573-1584.
47. Lu, C. S.; Anderson, L. C.; Morgan, M. S.; Fenske, R. A., Salivary concentrations of atrazine reflect free atrazine plasma levels in rats. *Journal of Toxicology and Environmental Health-Part A* **1998,** *53*, (4), 283-292.
48. Han, X.; Nabb, D. L.; Mingoia, R. T.; Yang, C. H., Determination of xenobiotic intrinsic clearance in freshly isolated hepatocytes from rainbow trout (Oncorhynchus mykiss) and rat and its application in bioaccumulation assessment. *Environmental Science & Technology* **2007,** *41*, (9), 3269-3276.
49. Gorge, G.; Nagel, R., Kinetics and metabolism of 14c-lindane and 14c-atrazine in early life stages of zebrafish (*Brachydanio-rerio*). *Chemosphere* **1990,** *21*, (9), 1125-1137.
50. Abbas, R. A physiologically based pharmacokinetic and pharmacodynamic model for paraoxon in rainbow trout. The Ohio State University, 1994.
51. Maxwell, D. M.; Lenz, D. E.; Groff, W. A.; Kaminskis, A.; Froehlich, H. L., The effects of blood flow and detoxification on in vivo cholinesterase inhibition by Soman in rats. *Toxicology and Applied Pharmacology* **1987,** *88*, (1), 66-76.
52. Saltelli, A.; Chan, K.; Scott, E. M., *Sensitivity Analysis*. John Wiley & Sons, Ltd ed.; New York, 2008.
53. Sobol, I. M.; Tarantola, S.; Gatelli, D.; Kucherenko, S. S.; Mauntz, W., Estimating the approximation errors when fixing unessential factors in global sensitivity analysis. *Reliability Engineering & System Safety* **2007,** *92*, 957-960.

54. R Core Team *R: A Language and Environment for Statistical Computing*, R Foundation for Statistical Computing: Vienna, Austria, 2019.
55. Soetaert, K.; Petzoldt, T.; Setzer, R. W., Solving Differential Equations in R: Package deSolve. *Journal of Statistical Software* **2010,** *33*, (9), 1-25.
56. Pujol, G.; Iooss, B.; Janon, A.; Boumhaout, K.; Da Veiga, S.; Delage, T.; Fruth, J.; Gilquin, L.; Guillaume, J.; Le Gratiet, L.; Lemaitre, P.; Nelson, B. L.; Monari, F.; Oomen, R.; Ramos, B.; Roustant, O.; Song, E.; Staum, J.; Touati, T.; Weber, F. *sensitivity: Global Sensitivity Analysis of Model Outputs*, 1.16.1; 2019.
57. Bois, F. Y., GNU MCSim: Bayesian statistical inference for SBML-coded systems biology models. *Bioinformatics* **2009,** *25*, 1453-1454.
58. Ling, M. P.; Liao, C. M.; Tsai, J. W.; Chen, B. C., A PBTK/TD Modeling-Based Approach Can Assess Arsenic Bioaccumulation in Farmed Tilapia (Oreochromis mossambicus) and Human Health Risks. *Integr. Environ. Assess. Manag.* **2005,** *1*, (1), 40-54.
59. Products, E. Panel o. P. P.; Residues, t.; Ockleford, C.; Adriaanse, P.; Berny, P.; Brock, T.; Duquesne, S.; Grilli, S.; Hernandez-Jerez, A. F.; Bennekou, S. H.; Klein, M.; Kuhl, T.; Laskowski, R.; Machera, K.; Pelkonen, O.; Pieper, S.; Smith, R. H.; Stemmer, M.; Sundh, I.; Tiktak, A.; Topping, C. J.; Wolterink, G.; Cedergreen, N.; Charles, S.; Focks, A.; Reed, M.; Arena, M.; Ippolito, A.; Byers, H.; Teodorovic, I., Scientific Opinion on the state of the art of Toxicokinetic/Toxicodynamic (TKTD) effect models for regulatory risk assessment of pesticides for aquatic organisms. *EFSA Journal* **2018,** *16*, (8), e05377.
60. Conolly, R. B.; Ankley, G. T.; Cheng, W.; Mayo, M. L.; Miller, D. H.; Perkins, E. J.; Villeneuve, D. L.; Watanabe, K. H., Quantitative Adverse Outcome Pathways and Their Application to Predictive Toxicology. *Environmental Science & Technology* **2017,** *51*, (8), 4661-4672.
61. Barron, M. G.; Plakas, S. M.; Wilga, P. C., CHLORPYRIFOS PHARMACOKINETICS AND METABOLISM FOLLOWING INTRAVASCULAR AND DIETARY ADMINISTRATION IN CHANNEL CATFISH. *Toxicology and Applied Pharmacology* **1991,** *108*, (3), 474-482.
62. Barron, M. G.; Plakas, S. M.; Wilga, P. C.; Ball, T., Absorption, tissue distribution and metabolism of chlorpyrifos in channel catfish following waterborne exposure. *Environmental Toxicology and Chemistry* **1993,** *12*, (8), 1469-1476.
63. Sultatos, L. G.; Murphy, S. D., Kinetic analyses of the microsomal biotransformation of the phosphorothioate insecticides chlorpyrifos and parathion. *Fundamental and Applied Toxicology* **1983,** *3*, (1), 16-21.
64. Freitas, A. P.; Santos, C. R.; Sarcinelli, P. N.; Silva, M. V.; Hauser-Davis, R. A.; Lopes, R. M., Evaluation of a Brain Acetylcholinesterase Extraction Method and Kinetic Constants after Methyl-Paraoxon Inhibition in Three Brazilian Fish Species. *Plos One* **2016,** *11*, (9).
65. Kardos, S. A.; Sultatos, L. G., Interactions of the Organophosphates Paraoxon and Methyl Paraoxon with Mouse Brain Acetylcholinesterase. *Toxicological Sciences* **2000,** *58*, (1), 118-126.
66. Sturm, A.; Radau, T. S.; Hahn, T.; Schulz, R., Inhibition of rainbow trout acetylcholinesterase by aqueous and suspended particle-associated organophosphorous insecticides. *Chemosphere* **2007,** *68*, (4), 605-612.
67. Carr, R. L.; Chambers, J. E., Kinetic analysis of the in vitro inhibition, aging, and reactivation of brain acetylcholinesterase from rat and channel catfish by paraoxon and chlorpyrifos-oxon. *Toxicology and Applied Pharmacology* **1996,** *139*, (2), 365-373.
68. Barron, M. G.; Charron, K. A.; Stott, W. T.; Duvall, S. E., Tissue carboxylesterase activity of rainbow trout. *Environmental Toxicology and Chemistry* **1999,** *18*, (11), 2506-2511.
69. Wogram, J.; Sturm, A.; Segner, H.; Liess, M., Effects of parathion on acetylcholinesterase, butyrylcholinesterase, and carboxylesterase in three-spined stickleback (Gasterosteus aculeatus) following short-term exposure. *Environmental Toxicology and Chemistry* **2001,** *20*, (7), 1528-1531.
70. Chuiko, G. M.; Podgornaya, V.; Zhelnin, Y. Y., Acetylcholinesterase and butyrylcholinesterase activities in brain and plasma of freshwater teleosts: cross-species and cross-family differences. *Comparative Biochemistry and Physiology B-Biochemistry & Molecular Biology* **2003,** *135*, (1), 55-61.

71. Timchalk, C.; Poet, T. S.; Hinman, M. N.; Busby, A. L.; Kousba, A. A., Pharmacokinetic and pharmacodynamic interaction for a binary mixture of chlorpyrifos and diazinon in the rat. *Toxicology and Applied Pharmacology* **2005,** *205*, (1), 31-42.
72. Küster, E., Cholin- and carboxylesterase activities in developing zebrafish embryos (Danio rerio) and their potential use for insecticide hazard assessment. *Aquatic Toxicology* **2005,** *75*, (1), 76-85.
73. Pan, C.; Yang, M.; Xu, H.; Xu, B.; Jiang, L.; Wu, M., Tissue bioconcentration and effects of fluoxetine in zebrafish (Danio rerio) and red crucian cap (Carassius auratus) after short-term and long-term exposure. *Chemosphere* **2018,** *205*, 8-14.
74. Coban, A.; Carr, R. L.; Chambers, H. W.; Willeford, K. O.; Chambers, J. E., Comparison of inhibition kinetics of several organophosphates, including some nerve agent surrogates, using human erythrocyte and rat and mouse brain acetylcholinesterase. *Toxicology letters* **2016,** *248*, 39-45.
75. Straus, D. L.; Chambers, J. E., Inhibition of acetylcholinesterase and aliesterases of fingerling channel catfish by chlorpyrifos, parathion, and S,S,S-tributyl phosphorotrithioate (DEF). *Aquatic Toxicology* **1995,** *33*, (3), 311-324.
76. Backhaus, T.; Altenburger, R.; Boedeker, W.; Faust, M.; Scholze, M.; Grimme, L. H., Predictability of the toxicity of a multiple mixture of dissimilarly acting chemicals to Vibrio fischeri. *Environmental Toxicology and Chemistry* **2000,** *19*, (9), 2348-2356.

Table lists

Table 1. Compound-specific parameters used in the PBTK model

Parameter	ATR	CPF	CPF-oxon
PC liver/blood	5.35[a]	5.27	2.59
PC brain/blood	1.94[a]	3.66	1.80
PC kidney/blood	1.47[a]	8.33	4.09
PC blood/water	X	X	122.85
PC richly perfused tissue/blood	1.47[a]	3.40	1.67
PC poorly perfused tissue/blood	1.18 [a]	1.25	0.62
PC skin/blood	1.47 [a]	2.31	1.14
PC gonads/blood	1.47 [a]	11.03	5.42
PC fat/blood	1.47 [a]	47.63	23.36
PC GIT/blood	5.47 [a]	3.71	1.83
$Cl_{hepatic}$ (mL/d/g liver)	0.024 [b]	_	_
V_{max} (µg/d/g)	–	3375[f] (TCP) 1305[f] (CPF-oxon)	3375
K_m (µg/mL)	_	50.3	50.3
Ke bile (d^{-1})	X	0[g]	_
Ke feces (d^{-1})	0.83[c]	0.83[c]	0.83
K_{BG} (d^{-1})	X	0	0
Ratio blood to plasma	1	1	1
Unbound fraction	0.74	X	1

Data were retrieved from : a-Gunkel and Streit [42], b-Han, et al. [44], c-Nichols, et al. [46], d-Lu, et al. [43], e-Grech, et al. [30], f-Lavado and Schlenk [39], g-Welling and de Vries [41] . The rest of the data was calculated using QSAR model in Grech, et al. [30]. Parameters with an X can be found in Table 2. All values presented here were not calibrated and fixed in the model.

Table 2. Compound-specific parameter estimates (mode and 95% confidence interval)

Parameter	ATR	CPF	CPF-oxon
Blood:Water partition coefficient (PC_{BW})	2.07 (1.95; 2.23)	1819 (1797; 7913)	-
Bile excretion rate (Ke_{bile}) (d^{-1})	5.76 (1.74;3.75)	-	-
Chemical rate constant from bile to GIT lumen (K_{BG}) (d^{-1})	1.80 ($8.60x10^{-3}$; $7.07x10^{-1}$)	-	-
Unbound fraction	-	$1.95x10^{-2}$ ($2.22x10^{-2}$; $1.52x10^{-1}$)	-
Bimolecular rate constant AChE ($nmol^{-1}.d^{-1}$)	$1.29x10^{-2}$ ($1.08x10^{-2}$; $2.20x10^{-2}$)	$1.08x10^{-4}$ ($1.69x10^{-5}$; $3.34x10^{-4}$)	$2.46x10^{-2}$ ($2.34x10^{-2}$; $6.31x10^{-2}$)
Bimolecular rate constant CEs ($nmol^{-1}.d^{-1}$)	$7.08x10^{-3}$ ($5.59x10^{-3}$; $1.23x10^{-2}$)	$3.14x10^{-6}$ ($2.90x10^{-7}$; $2.31x10^{-5}$)	$2.42x10^{-2}$ ($1.19x10^{-2}$; $2.59x10^{-2}$)

Table 3. Toxicodynamic parameter estimates (mode and 95% confidence interval)

Parameter	Brain	Muscle	Liver
Initial quantity of AChE (nmol.kg BW^{-1})	$4.17x10^{-4}$ ($3.47x10^{-4}$; $1.67x10^{-3}$)	$8.31x10^{-3}$ ($1.96x10^{-3}$; $9.63x10^{-3}$)	$1.37x10^{-5}$ ($6.96x10^{-6}$; $3.38x10^{-5}$)
Initial quantity of CEs (nmol.kg BW^{-1})	$1.19x10^{-2}$ ($4.96x10^{-3}$; $2.46x10^{-2}$)	97.1 (74.5; 110)	$6.88x10^{-1}$ ($3.31x10^{-1}$; 1.50)

Figure list

Figure 1. Potential relation between effects of atrazine and chlorpyrifos. Potential synergistic effect is symbolized in red.

Figure 2. Predicted atrazine concentrations in the whole zebrafish compared to the observation from Gorge and Nagel. The solid line represents the model predictions, dots represent the mean concentration in two juveniles (n=47) and the grey area is the 95% prediction interval, computed from the posterior distributions. These simulations were made using a sample based on every iteration of the last 3333 of each of the three MCMC chains.

Figure 3. Comparison between chlorpyrifos concentrations measured in fathead minnow (µg/g fish) and model predictions. Dotted lines represent the 3-fold and 10-fold changes. Experimental datasets used are indicated in legend. Data correspond to whole body concentration. Credibility intervals were too narrow to be represented.

Figure 4. Comparison between esterase inhibition (acetylcholine esterase in black and carboxylesterase in grey) reported by Xing *et al*. (2010) in common carp versus model predictions for 40-day-exposition (filled points) to (a, b) atrazine and to (c, d) chlorpyrifos followed by a 20-day-depuration (empty points). The inhibition in the brain, respectively in the muscle, are presented in (a) and (c), respectively (b) and (d). Solid grey line represents the identity line and 95% credibility intervals are represented, computed from a sample based on the posterior distribution.

Figure 5. Comparison between esterase inhibition (acetylcholine esterase in black and carboxylesterase in grey) reported by Xing *et al*. (2010) in common carp versus model predictions for 40-day-exposition (filled points) to a mixture of atrazine and chlorpyrifos followed by a 20-day-depuration (empty points). The inhibition in the brain, respectively in the muscle, is presented in panel (a), respectively (b). Solid grey line represents the identity line and 95% credibility intervals are represented, computed from a sample based on the posterior distribution.

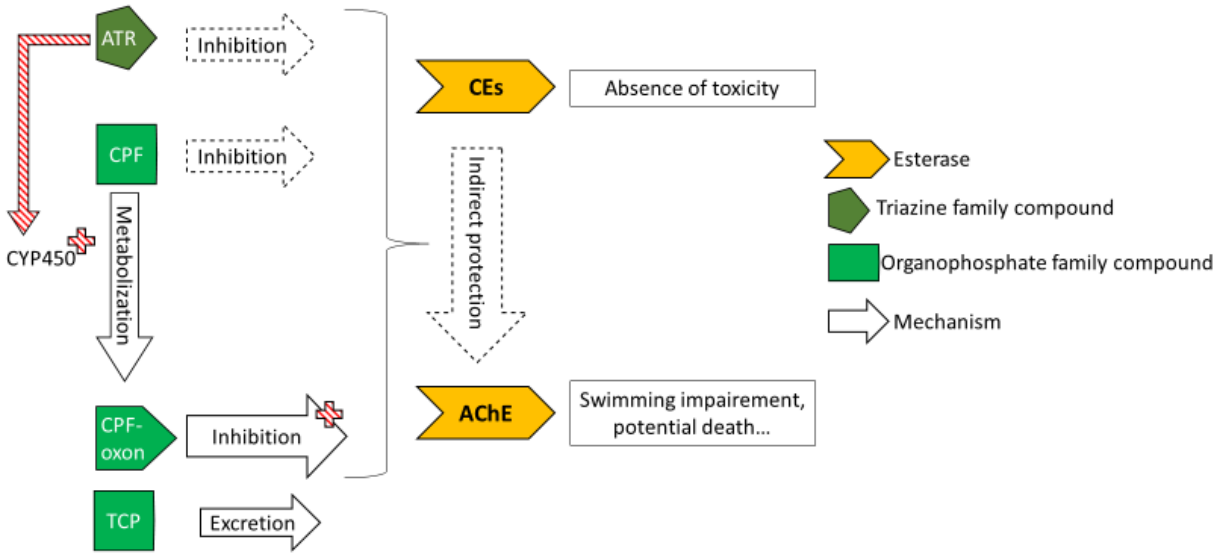

Figure 1. Potential relation between effects of atrazine and chlorpyrifos. Potential synergistic effect is symbolized in red.

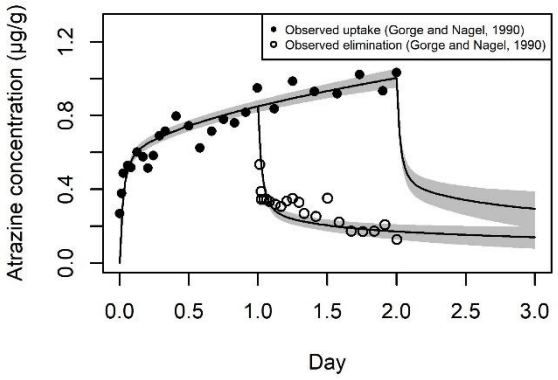

Figure 2. Predicted atrazine concentrations in the whole zebrafish compared to the observation from Gorge and Nagel. The solid line represents the model predictions, dots represent the mean concentration in two juveniles (n=47) and the grey area is the 95% prediction interval, computed from the posterior distributions. These simulations were made using a sample based on every iteration of the last 3333 of each of the three MCMC chains.

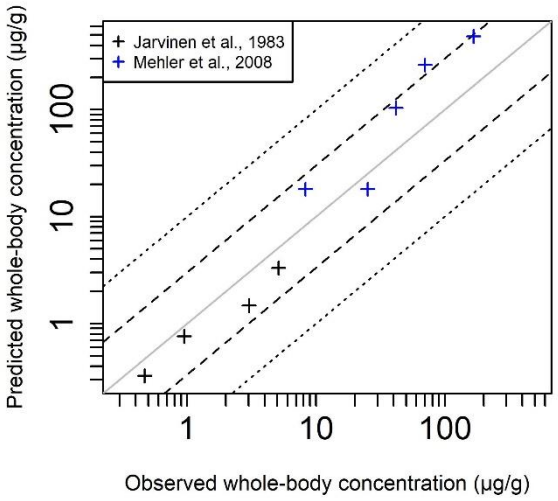

Figure 3. Comparison between chlorpyrifos concentrations measured in fathead minnow (µg/g fish) and model predictions. Dotted lines represent the 3-fold and 10-fold changes. Experimental datasets used are indicated in legend. Data correspond to whole body concentration. Credibility intervals were too narrow to be represented.

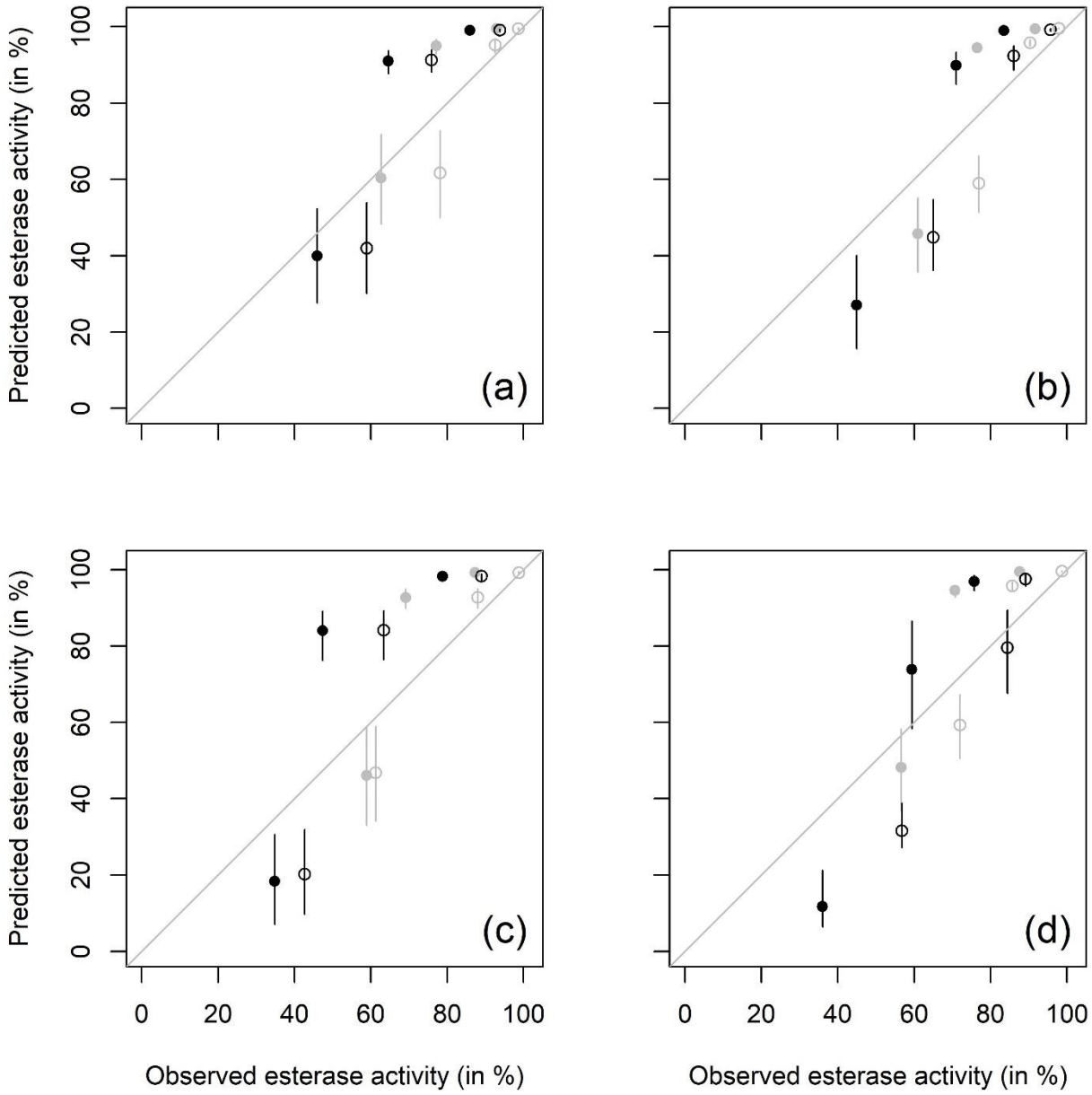

Figure 4. Comparison between esterase inhibition (acetylcholine esterase in black and carboxylesterase in grey) reported by Xing *et al*. (2010) in common carp versus model predictions for 40-day-exposition (filled points) to (a, b) atrazine and to (c, d) chlorpyrifos followed by a 20-day-depuration (empty points). The inhibition in the brain, respectively in the muscle, are presented in (a) and (c), respectively (b) and (d). Solid grey line represents the identity line and 95% credibility intervals are represented, computed from a sample based on the posterior distribution.

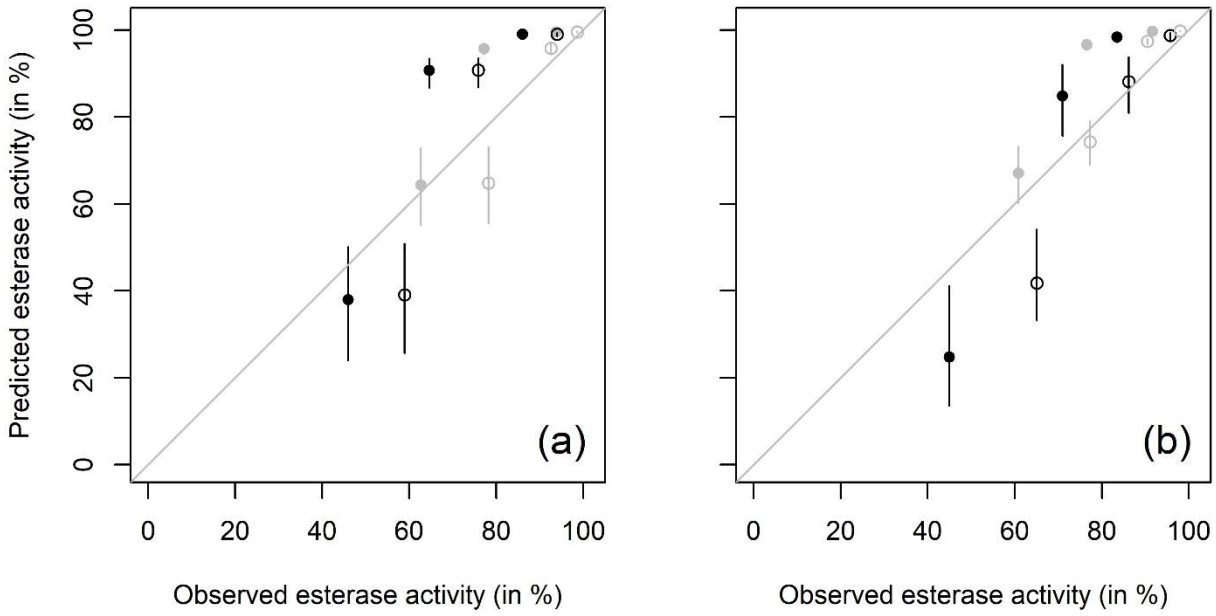

Figure 5. Comparison between esterase inhibition (acetylcholine esterase in black and carboxylesterase in grey) reported by Xing *et al*. (2010) in common carp versus model predictions for 40-day-exposition (filled points) to a mixture of atrazine and chlorpyrifos followed by a 20-day-depuration (empty points). The inhibition in the brain, respectively in the muscle, is presented in panel (a), respectively (b). Solid grey line represents the identity line and 95% credibility intervals are represented, computed from a sample based on the posterior distribution.

Supporting information to “Modelling acetylcholine esterase inhibition resulting from exposure to a mixture of atrazine and chlorpyrifos using a physiologically-based kinetic model in fish”

Contents

1. Model structure

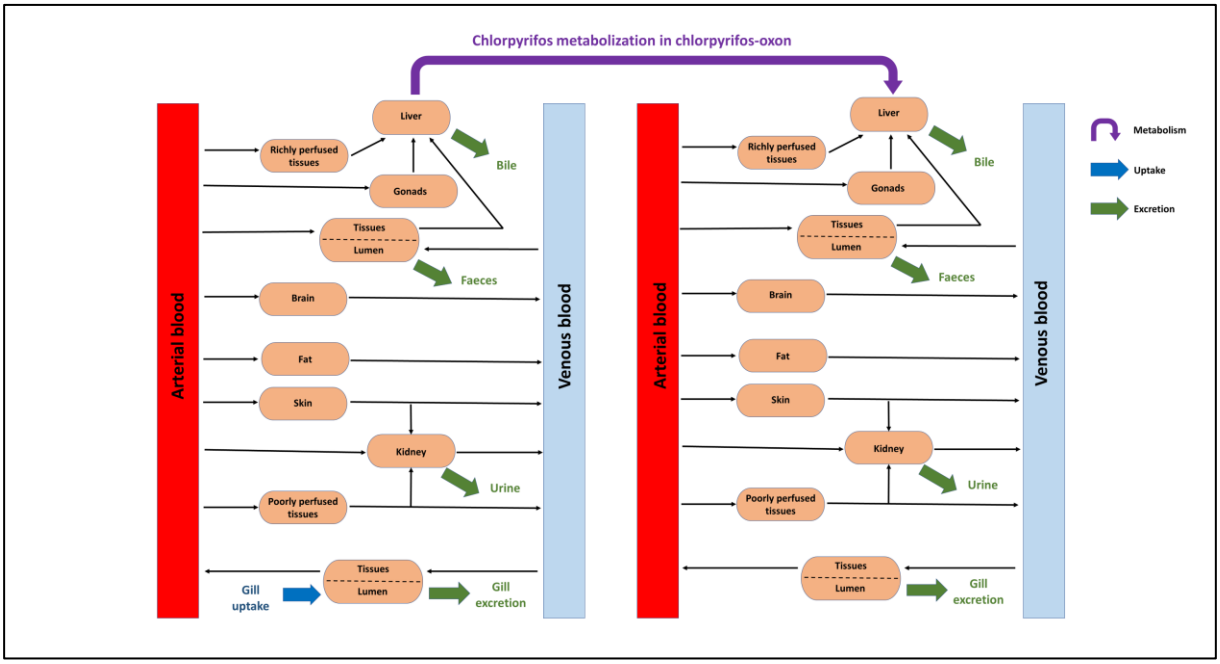

Figure S1. Schematic description of the PBK model developed for rainbow trout, zebrafish, fathead minnow, and stickleback. Metabolism, uptake and excretion sites are represented in purple, blue, and green, respectively.

The PBTK model used is based on the generic model developed by Grech, et al. [1]. This model has been successfully applied to four different species including rainbow trout, zebrafish, fathead minnow and threespine stickleback. It comprises twelve well-mixed blood flow limited compartments:

arterial and venous blood, gills, gastrointestinal tract (GIT), skin, kidney, fat, liver, gonads, brain, poorly perfused tissues (PPT), and richly perfused tissues (RPT). Cardiac output, oxygen consumption rate, and afferent oxygen concentration are modulated by temperature by using Arrhenius' function. It also includes a growth sub-model based on DEB theory [2], depending on temperature and food level. Absorption can be driven by GIT or gills. In terms of excretion, branchial, urinary, fecal, and biliary excretion routes have been modeled. Physiological parameter values were subject to an extensive literature search.

2. Model parameterization

2.1. Description of the TK and TD data available from the literature

An extensive search in literature was carried out using relevant keywords, and various combinations of those keywords:

“atrazine”, “chlorpyrifos”, “fish”, “toxicokinetic”, “toxicodynamic”, “acetylcholinesterase inhibition”, “PBTK”, “in vivo”, “in vitro”, “metaboli*”, “excretion”, “accumulation”, “distribution”,

“absorption”. TK and TD data obtained *in vivo* in fish exposed to ATR, CPF, or both was collected from the literature in a total of 12 publications (see Table S1 in SI*)*. The data had been obtained in 8 different fish species. Three publications reported TK data only [3-5]. The nine others were reported *in vivo* AChE inhibition in a context of exposure to CPF, ATR, a mixture of both or pre-exposure to ATR followed by CPF [6-13]. The internal concentrations of ATR, CPF or CPF-oxon were measured at single or multiple timepoints in whole body or in organs. Activity of AChE was determined in muscle, liver or brain. In addition, CEs activity was also measured in three studies. Among these studies, Xing et al. (2010) provided a complete description of the exposure scenarios as well as a study of both ATR and CPF, and a mixture of both, with the same experimental design. Consequently, this dataset was selected to develop our model. The other datasets were not used in the present study as these authors used very small juveniles, *e.g.* trout weight under 5 g in 3 on 4 publications, and they do not report data on the chemical TK. Therefore, these data were considered to be outside of our application domain. Indeed, even if the model can be used with data from juveniles, those juveniles were considered to be too small, i.e. too different from adults. In addition to *in vivo* data, *in vitro* data from the literature was used for the TD sub-model (Table S2 and S3 in SI). The data had been obtained on mice, rat and trout [14-17].

Table S1. Summary on experiment data on chlorpyrifos and atrazine in fish

Study reference	Species	Fish per dose	Initial weigth (g)	Aquarium volume (L)	Dose ATR (µg/L)	Dose CPF (µg/L)	Exposure scenario	Timepoints of measurements	Tissues where concentration is measured	Tissues where esterase inhibition is measured	Esterase inhibition
Jarvinen, et al. [12]	Pimephales promelas	2	0.2	41	_	2.68,1.21,0.63,0.27, 0.12	60 d (continuous)	End point measurement	Whole body		_
Mehler, et al. [6]		30	0.05	4	_	339,201, 105,53, 25	2 d (static)	End point measurement	Whole body	Whole body	AChE
Wacksman, et al. [8]		30	0.5	9.5	0, 1000		ATR for 2 d then CPF 2 d (semi-static; pulse-dose)	End point measurement	_	Brain	AChE
					1000	1.03, 8.87, 47.14			_		
Sandahl and Jenkins [7]	Oncorhynchus mykiss	50	3.8	1.5		0.00,0.625, 1.25 ,1.875 ,2.50	4 d (static)	End point measurement	_	Brain	AChE
Sturm, et al. [10]		10	14.6	30		0.1, 0.3, 1, 3.3	1 h (continuous)	End point measurement	_	Brain, muscle	AChE
Gorge and Nagel [5]	Danio rerio	150	0.02	0.5	135		1 d,2 d (static)	47-point measurements	Whole body, repeated		_
Schmidel, et al. [11]		12	NS	3	0, 10, 1000		14 d (continuous)	End point measurement		Brain, muscle	AChE
Barron, et al. [4]	Ictalurus punctatus	21	300	40		12	4 d (static)	4-point measurements		Whole body	CES AChE
Gunkel and Streit [3]	Coregonus fera	NS	4	300	50		1 d (static)	End point measurement	Blood, muscle, gall bladder, liver, stomach, intestine, brain, remainder		_

Xing, et al. [13]	Cyprinus carpio	20	190	200	4.28, 42.8, 428		40 d (semi-static ; 20d depuration)	2-point measurements		Brain, muscle	CES AChE
						1.16, 11.6, 116					
					1.13, 11.3, 113						
Sandahl, et al. [18]	Oncorhynchus kisutch	15	0.7	30		0.00,0.625, 1.25 ,1.875 ,2.50	4 d (static)	End point measurement		Brain, muscle	AChE
Wheelock, et al. [9]	Oncorhynchus tshawytscha	10	4	4		0, 1.2, 7.3	4 d	End point measurement		Brain, muscle, liver	CES AChE

2.2. Toxicodynamic parameter values collected from the literature

Table S2. Toxicodynamic parameter values for enzyme synthesis and degradation collected from the literature. Source and value for the different parameters are listed. Only the degradation rates of AChE in rainbow trout were used in the model.

Enzyme	Unit	brain	muscle	liver	Reference
AChE synthesis rate in rainbow trout	nmol/d	11.0[a]	18.9[a]	7.95[b]	a16 b19
AChE synthesis rate in rat		0.0336			20, 21
AChE degradation rate in rainbow trout	(/d)	$1.75x10^{-3}$ [a]	$1.40x10^{-2}$ [a]	0.112[b]	a16 b 19
AChE degradation rate in rat		0.24[c]		0.24[d]	c21, 22 d14, 23

Table S3. Data used for the toxicodynamic parameterization of initial enzyme quantities

	Brain	**Muscle**	**Liver**	**Reference**
Initial CEs in 250g rats (nmol)	1.60	289*	460	[24, 25]. * or 65 depending on the publication
Initial AChE in 250g rats (nmol)	0.11	0.843	0.009	
Relative organ weight in rat	0.0057	0.404	0.0366	[26]
Relative organ weight PBTK model for fathead minnow	0.0112	0.673	0.0218	
Protein content in rat (mg/g tissue)	**104[a]** 55.3[g] 60.4[h]	164[b]	210[c]	**a27** b 28 c 29 g 17 h 30
Protein content in fish (mg/g tissue)	**91.7 [d]** 39.8 [i] 41.5[j] 38.9[k] 40.6[l] 81[m]	142 [e]	150 [f]	**[d] shortspine thornyhead (*Sebastolobus alascanus)* [31]** [e] rainbow trout [32] [f] rainbow trout [33] [i] trout [17] [j] trout [30] [k] fathead minnow [17] [l] fathead minnow [30] [m] *Scorpaena guttata* [31]
Initial CEs in fathead minnow (nmol/g BW)	0.0111	1.48	0.783	calculated
Initial CEs in rainbow trout (nmol/g BW)	0.00485	1.66	0.524	calculated
Initial AChE in fathead minnow (nmol/g BW)	$7.63x10^{-4}$	0.00432	$1.53x10^{-5}$	calculated
initial AChE in rainbow trout (nmol/min/mg prot)	32.9	8.7	2.89	[16, 19]
initial AChE in rainbow trout (nmol/g BW)	14.8	831	6.33	[16, 19] calculated using data from Abbas and protein content and relative organ weight

2.3. Physiological parameters in the PBTK model

Physiological parameters for toxicokinetics in rainbow trout and fathead minnow were collected by [1] and are reported for fathead minnow.

Table S4: Physiological parameters used in the PBTK model for fathead minnow, as proposed by [1].

Parameters (fraction)	value
Relative weight	
Adipose tissues	0.02
Blood	0.02
Brain	0.01
GIT	0.10
Gonads	0.01
Kidney	0.002
Liver	0.02
PPT	0.67
RPT	0.03
Skin	0.10
Relative blood flow	
Adipose tissues	0.01
Brain	0.04
GIT	0.17
Gonads	0.01
Kidney	0.02
Liver	0.02
PPT	0.54
RPT	0.13
Skin	0.06
PPT blood flow to kidney (α_{Fpp})	0.60
Skin blood flow to kidney (α_{Fs})	0.90
Relative water content	
Adipose tissues	0.03
Brain	0.75
GIT	0.77
Gonads	0.52
Kidney	0.49
Liver	0.65
PPT	0.81
RPT	0.53
Skin	0.76
Relative lipid content	
Adipose tissues	1.00
Brain	0.07
GIT	0.07
Gonads	0.22
Kidney	0.17
Liver	0.10
PPT	0.02
RPT	0.07
Skin	0.05

2.4. MCMC Calibration

Parameters were calibrated using MonteCarlo Markov Chains, with 3 chains of 100000 iterations each. To avoid correlations between parameters, two toxicokinetic parameters were calibrated using an intermediate ratio. Calibration was carried out on those ratio (Eq.1 for CPF and Eq.2 for ATR). Convergence was assessed in R 3.6.1 [34] with the package coda [35] by checking that autocorrelations were low (i.e. that the chains were well mixed), that estimates lay well within the prior boundaries, and that the Gelman-Rubin index [36] was close to 1.

$$\mathrm{UF} = \mathrm{PC}_{bw} \times Ratio_{bw\_UF} \quad (1)$$

$$\mathrm{K}_{BG} = \mathrm{Ke}_{bile} \times Ratio_{Kbg\_Kebile} \quad (2)$$

Table S5. Prior distributions and references for calibrated parameters

Parameter	Prior distribution	Reference
ATR Blood:Water partition coefficient (PC_{BW})	Normal (2.3,0.1)	Gunkel and Streit [3]
Bile excretion rate (Ke_{bile}) (d^{-1})	Uniform (0,50)	-
Ratio K_{BG} _/ Ke_{bile}	Uniform (0,1)	-
CPF Blood:Water partition coefficient (PC_{BW})	LogNormal (1000,3)	[1]
Ratio bw_UF	Uniform (1E3,1E7)	-
Bimolecular rate constant AChE ($nmol^{-1}.d^{-1}$)	Uniform (1E-12,10)	-
Bimolecular rate constant CEs ($nmol^{-1}.d^{-1}$)	Uniform (1E-12,10)	-
Initial quantity of AChE (nmol.kg BW^{-1})		See Table 3 for details
Brain		
	LogNormal ($7.63x10^{-4}$,1.5)	
Muscle		
	LogNormal (0.00432,1.5)	
Liver		
	LogNormal ($1.53x10^{-5}$,1.5)	
Initial quantity of AChE (nmol.kg BW^{-1})		See Table 3 for details
Brain		
	LogNormal (0.0111,1.5)	
Muscle		
	LogNormal (1.48,1.5)	
Liver		
	LogNormal (0.783,1.5)	

All bimolecular rates were set to the same prior value because of the lack of data on compound-specific toxicodynamics.

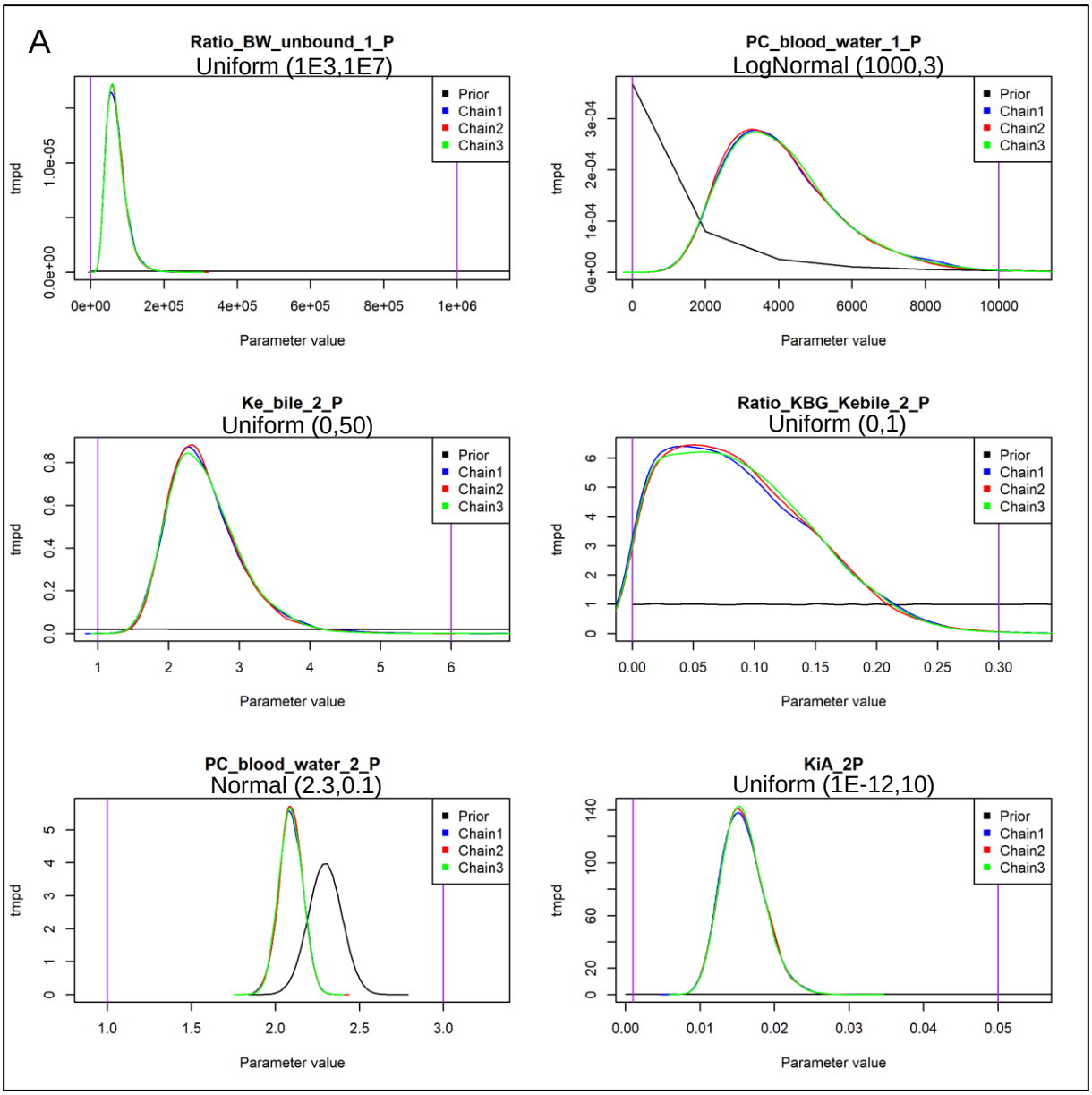
A
Ratio_BW_unbound_1_P
Uniform (1E3,1E7)
PC_blood_water_1_P
LogNormal (1000,3)
Ke_bile_2_P
Uniform (0,50)
Ratio_KBG_Kebile_2_P
Uniform (0,1)
PC_blood_water_2_P
Normal (2.3,0.1)
KiA_2P
Uniform (1E-12,10)
Prior
Chain1
Chain2
Chain3
tmpd
Parameter value

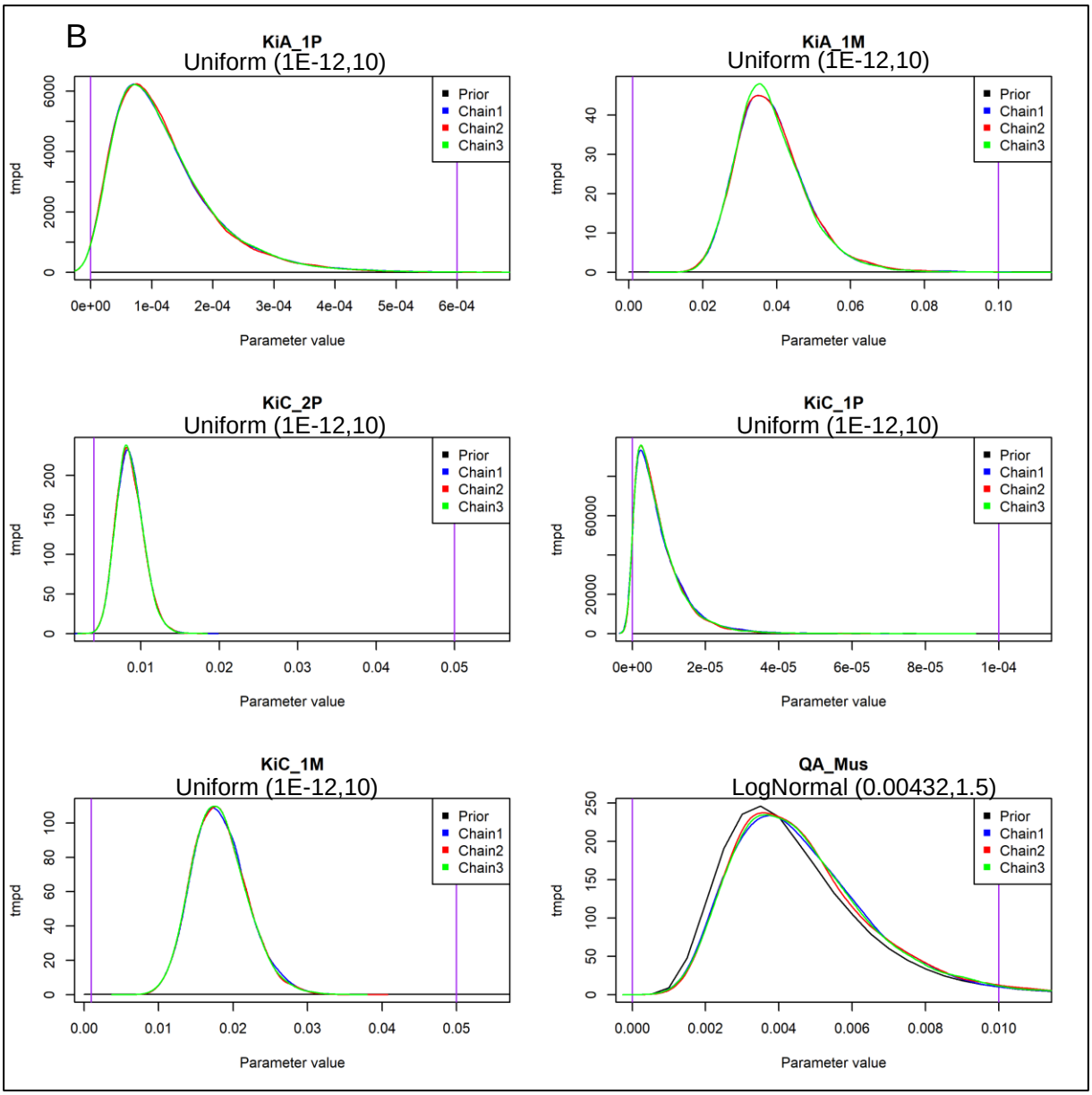
B
KiA_1P
Uniform (1E-12,10)
KiA_1M
Uniform (1E-12,10)
KiC_2P
Uniform (1E-12,10)
KiC_1P
Uniform (1E-12,10)
KiC_1M
Uniform (1E-12,10)
QA_Mus
LogNormal (0.00432,1.5)
Prior
Chain1
Chain2
Chain3
tmpd
Parameter value

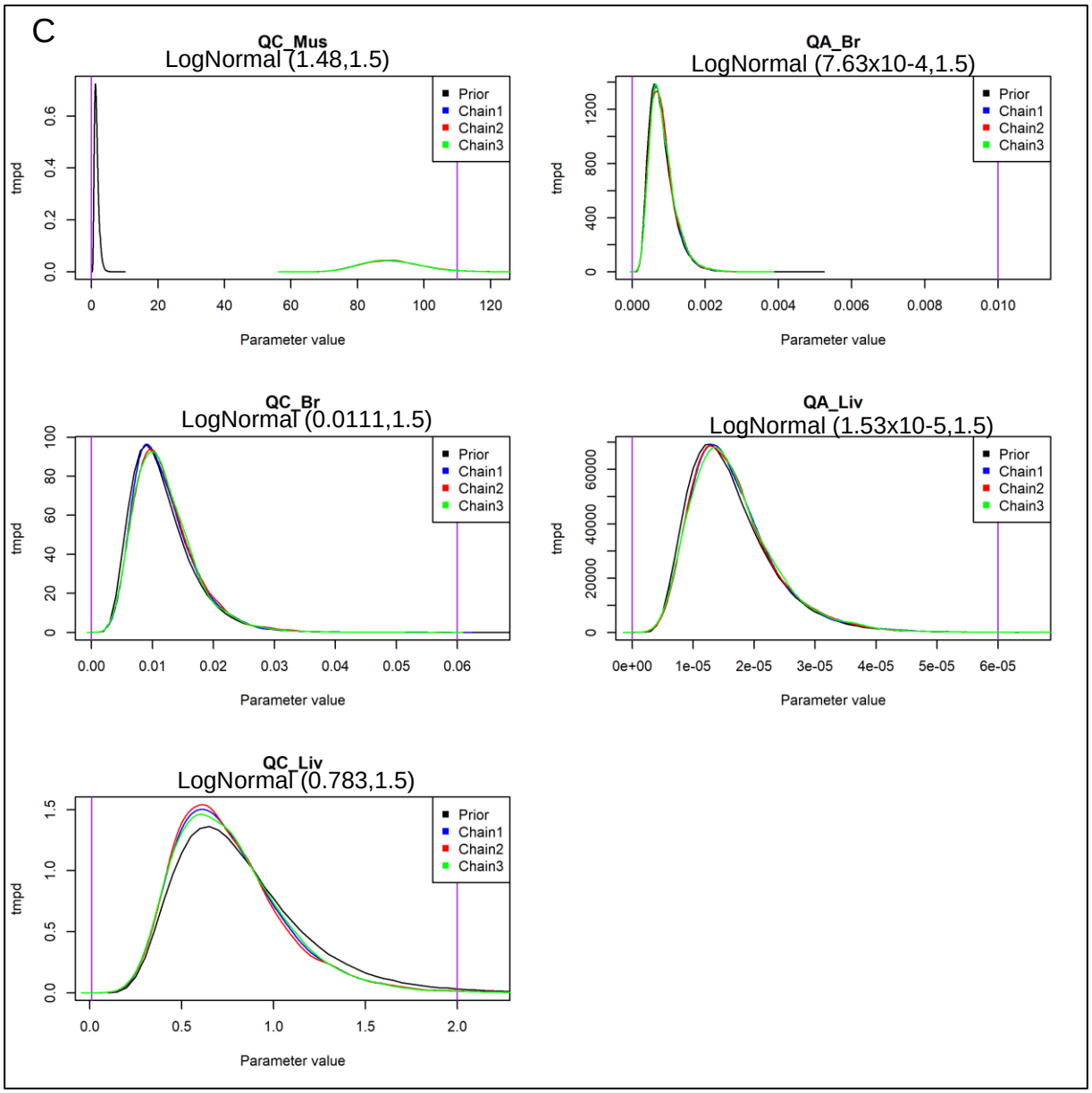

Figure S2: comparison between prior and posterior distributions for the 17 calibrated parameters (panel A and B, six parameters and panel C, five parameters). Prior distribution is represented in black and each of the three chains is represented in blue, red and green. Bounds in purple were placed arbitrarily to ease the reading. Each prior distribution can be found below each parameter name.

On Figure S2, the convergence of the three chains can be checked visually, so as the little deviation between priors and posteriors when given normal and lognormal distribution. Each chain contains the 50000 last values of each calibrated parameters.

3. Sensitivity analysis

A sensitivity analysis of AChE and CEs enzyme inhibition in brain and muscle was performed, according to the exposure scenario used with carps used by [13] after 40 days exposure to either ATR or CPF and after 20 days depuration, and using the variance-based Sobol method [37, 38]. 65 chemical-specific parameters were taken into account with uniform

distributions ±10% of the parameter values obtained by the calibration of TK and TD parameters.

Table S6. Mean parameter values used in the sensitivity analysis

Parameter	Mean value
Ratio_BW_unbound_1_P	93366.9
Ratio_blood_plasma_1_P	1
Unbound_fraction_2_P	0.74
Ratio_blood_plasma_2_P	1
Unbound_fraction_1_M	1
Ratio_blood_plasma_1_M	1
PC_blood_water_1_P	1818.74
PC_liver_1_P	5.26561
PC_gonads_1_P	11.032237
PC_brain_1_P	3.661017
PC_fat_1_P	47.637959
PC_skin_1_P	2.307105
PC_git_1_P	3.71117
PC_kidney_1_P	8.329398
PC_rp_1_P	3.395132
PC_pp_1_P	1.254078
PC_blood_water_2_P	2.06467
PC_liver_2_P	5.35
PC_gonads_2_P	1.47
PC_brain_2_P	1.94
PC_fat_2_P	1.47
PC_skin_2_P	1.47
PC_git_2_P	5.47
PC_kidney_2_P	1.47
PC_rp_2_P	1.47
PC_pp_2_P	1.18
PC_blood_water_1_M	122.85
PC_liver_1_M	2.59
PC_gonads_1_M	5.42
PC_brain_1_M	1.8013
PC_fat_1_M	23.36
PC_skin_1_M	1.14
PC_git_1_M	1.83
PC_kidney_1_M	4.09
PC_rp_1_M	1.6692102
PC_pp_1_M	0.62
Km_1_P	50.29
Vmax_1_P	1305
Cl_liver_2_P	0.024
Km_1_TCP	50.29
Vmax_1_TCP	3375
Km_1_M	50.29

Vmax_1_M	1305
Ke_feces_1_P	0.83
Ke_feces_1_M	0.83
Ke_feces_2_P	0.83
urine_rate	2982
Kd_AChE_Brain	0.0017544
Kd_AChE_Muscle	0.013992
Kd_AChE_Liver	0.1116
Ki_AChE_1_M	0.024634
Ki_AChE_2_P	0.0129429
Ki_AChE_1_P	0.000107842
Kd_CaE_Brain	0.0017544
Kd_CaE_Muscle	0.013992
Kd_CaE_Liver	0.1116
Ki_CaE_1_M	0.0242113
Ki_CaE_2_P	0.00708234
Ki_CaE_1_P	3.15E-06
Q_enz_AChE_init_Brain	0.00041735
Q_enz_AChE_init_Muscle	0.00831161
Q_enz_AChE_init_Liver	0.000013725
Q_enz_CaE_init_Brain	0.0119196
Q_enz_CaE_init_Muscle	97.1347
Q_enz_CaE_init_Liver	0.688188

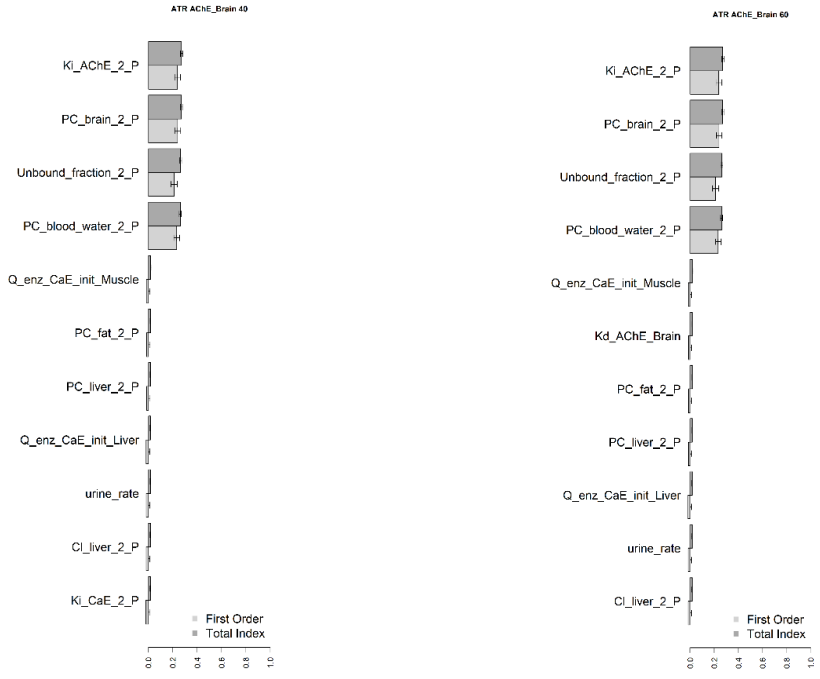

Figure S3: Sensitivity analysis on AChE inhibition in brain for an exposure of 40d to atrazine and a depuration of 20d following Xing et *al*. (2010). The top ten most influential parameters are represented.

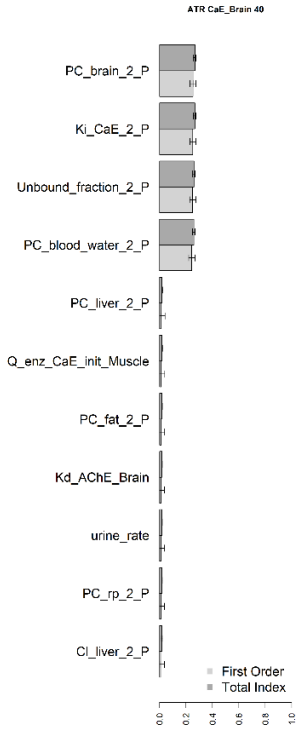

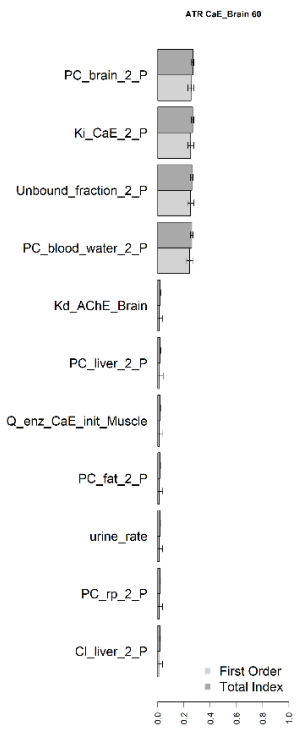

Figure S4: Sensitivity analysis on CEs inhibition in brain for an exposure of 40d to atrazine and a depuration of 20d following Xing et *al*. (2010). The top ten most influential parameters are represented.

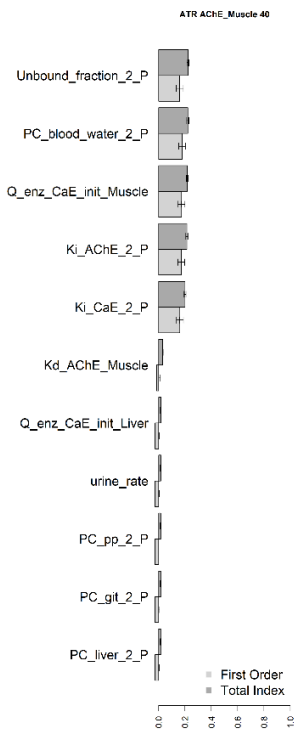

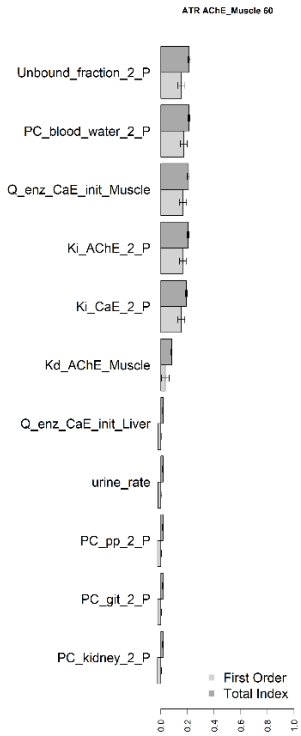

Figure S5: Sensitivity analysis on AChE inhibition in muscle for an exposure of 40d to atrazine and a depuration of 20d following Xing et *al*. (2010). The top ten most influential parameters are represented.

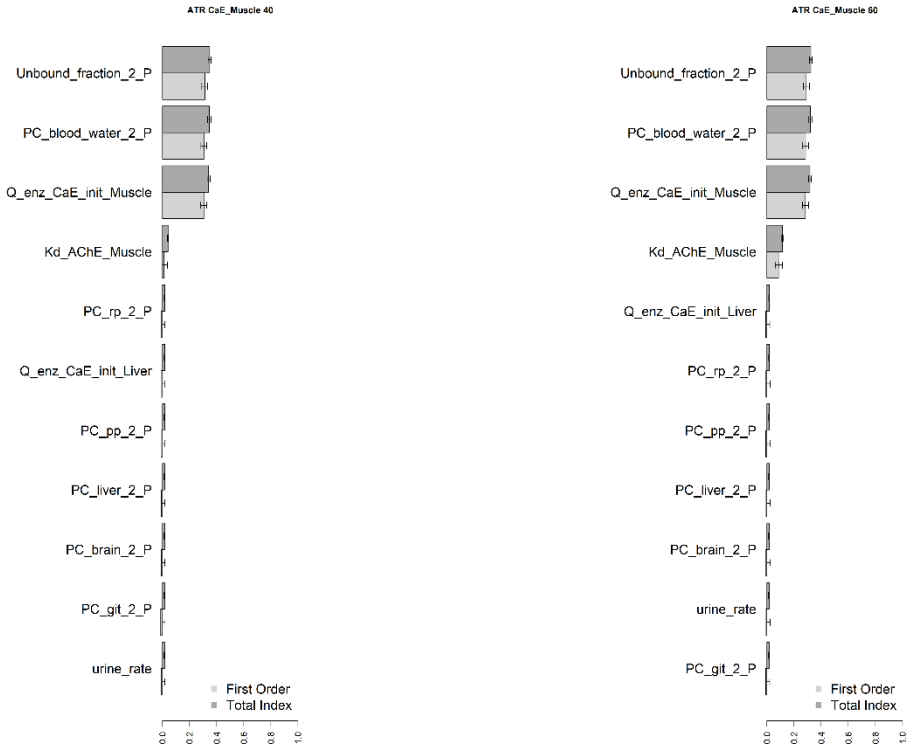

Figure S6: Sensitivity analysis on CEs inhibition in muscle for an exposure of 40d to atrazine and a depuration of 20d following Xing et *al*. (2010). The top ten most influential parameters are represented.

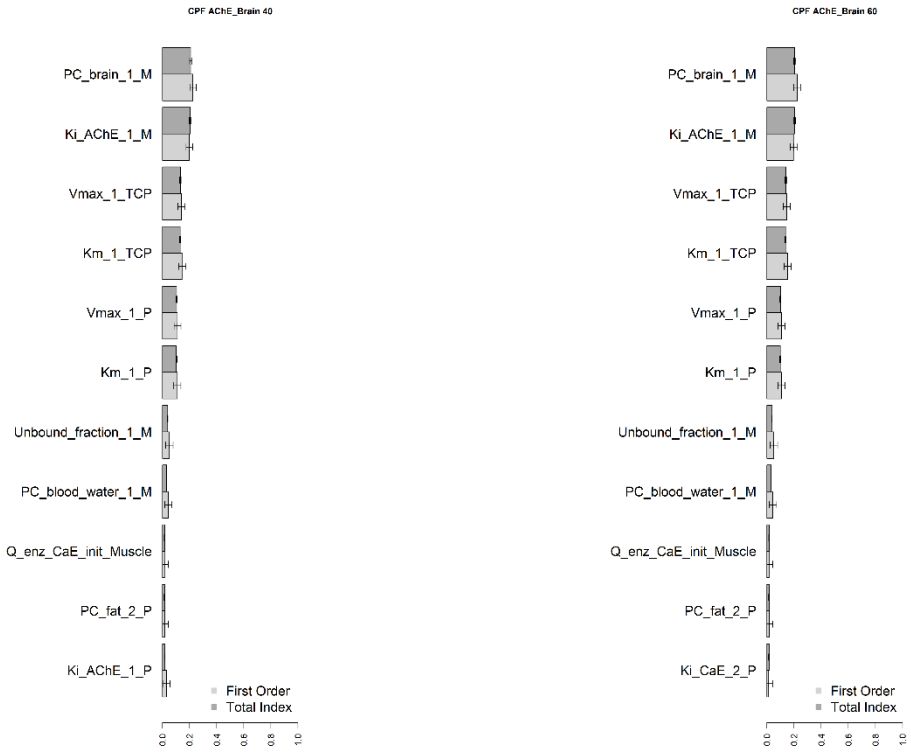

Figure S7: Sensitivity analysis on AChE inhibition in brain for an exposure of 40d to chlorpyrifos and a depuration of 20d following Xing et *al*. (2010). The top ten most influential parameters are represented.

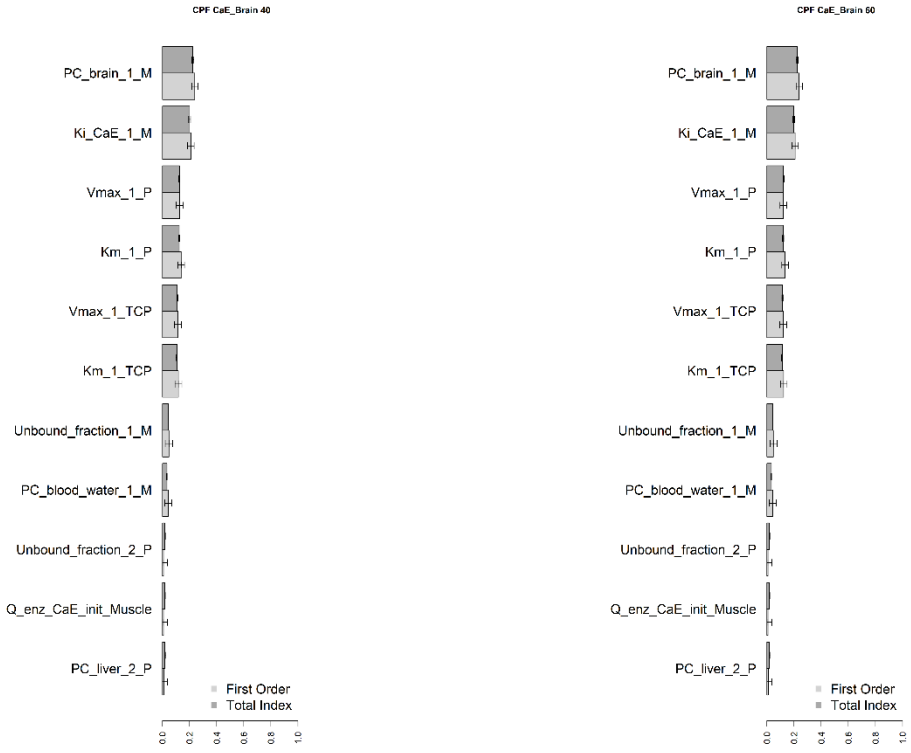

Figure S8: Sensitivity analysis on CEs inhibition in brain for an exposure of 40d to chlorpyrifos and a depuration of 20d following Xing et *al*. (2010). The top ten most influential parameters are represented.

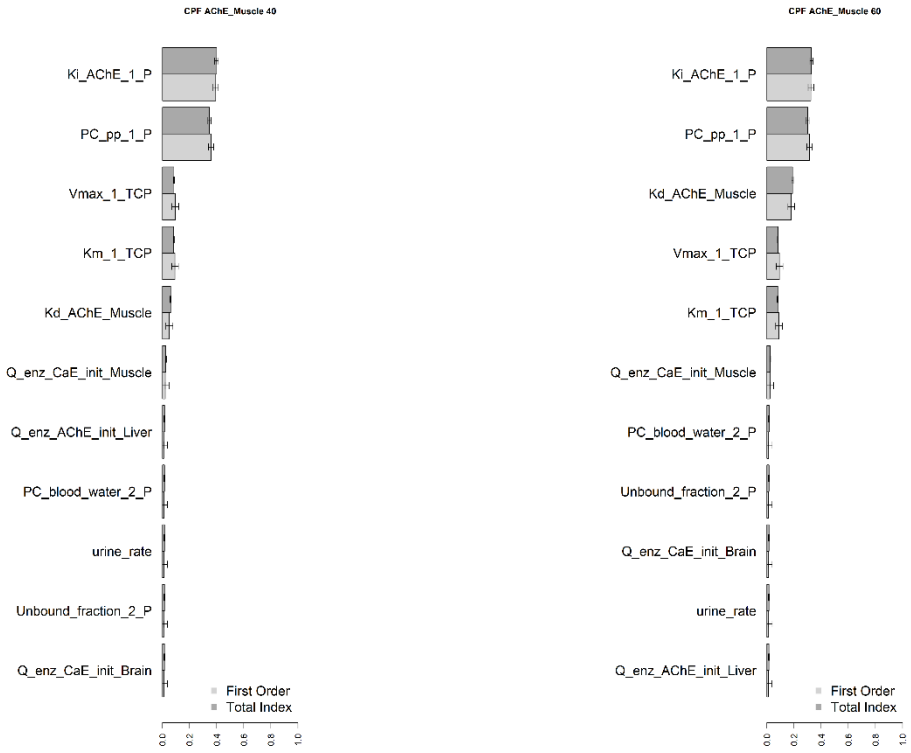

Figure S9: Sensitivity analysis on AChE inhibition in muscle for an exposure of 40d to chlorpyrifos and a depuration of 20d following Xing et *al*. (2010). The top ten most influential parameters are represented.

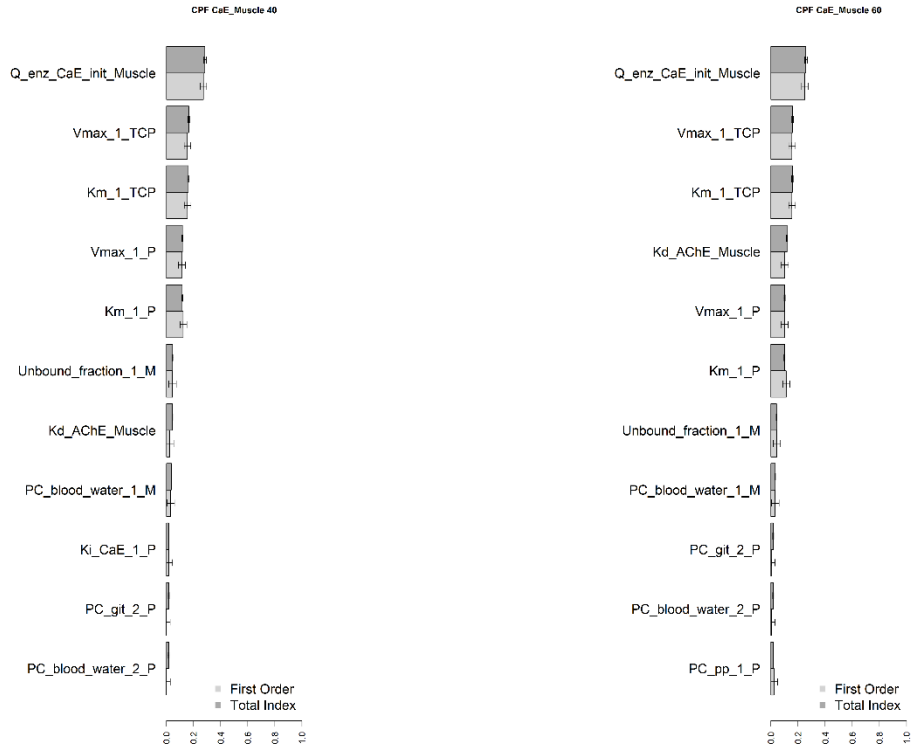

Figure S10. Sensitivity analysis on CEs inhibition in muscle for an exposure of 40d to chlorpyrifos and a depuration of 20d following Xing et *al*. (2010). The top ten most influential parameters were represented.

4. Results of the calibration

4.1. Toxicokinetic calibration

Table S7: Estimates of chemical-specific TK parameters when TK and TD were calibrated separately.

Parameter	ATR	CPF	CPF-oxon
Blood:Water partition coefficient (PC_{BW})	2.22 (2.09,2.36)	2009 (1026,5502)	-
Bile excretion rate (Ke_{bile}) (d^{-1})	2.48 (1.81,4.12)	-	-
Chemical rate constant from bile to GIT lumen (K_{BG}) (d^{-1})	$3.41x10^{-4}$ ($7.48x10^{-3}$,6.29 $x10^{-1}$)	-	-
Unbound fraction	-	$3.84x10^{-2}$ ($1.41x10^{-2}$, $1.07x10^{-1}$)	-

4.2. Toxicodynamic calibration

Table S8: Estimates of chemical-specific TD parameters when TK and TD were calibrated separately.

Parameter	ATR	CPF	CPF-oxon
Bimolecular rate constant AChE ($nmol^{-1}.d^{-1}$)	$1.58x10^{-2}$ ($1.02x10^{-2}$, $2.06x10^{-2}$)	$3.93x10^{-5}$ ($9.60x10^{-6}$,1.23 $x10^{-3}$)	$4.14x10^{-2}$ ($2.42x10^{-2}$, $6.33x10^{-2}$)
Bimolecular rate constant CEs ($nmol^{-1}.d^{-1}$)	$6.88x10^{-3}$ ($5.27x10^{-3,}$ $1.17x10^{-2}$)	$5.67x10^{-6}$ ($1.81x10^{-7}$, $1.10x10^{-5}$)	$1.78x10^{-2}$ ($1.22x10^{-2}$, $2.65x10^{-2}$)

Table S9: Estimates of physiological TD parameters when TK and TD were calibrated separately.

Parameter	Brain	Muscle	Liver
Initial quantity of AChE (nmol.kg BW^{-1})	5.22x10^{-4} (3.45x10^{-4}, 1.68x10^{-3})	3.51x10^{-3} (1.96x10^{-3},9.46x10^{-3})	1.20x10^{-5} (6.91x10^{-6}, 3.41x10^{-5})
Initial quantity of CEs (nmol.kg BW^{-1})	1.21x10^{-2} (5.04x10^{-3}, 2.42x10^{-2})	125 (78,115)	6.82x10^{-1} (3.29x10^{-1},1.49)

4.3. Predicted dose-responses

The dose-response relationships predicted with the PBTK-TD model and resulting from exposure to ATR, CPF, or a mixture of both were compared with observations made by Xing et al in carp (Figure S11 and Figure S12).

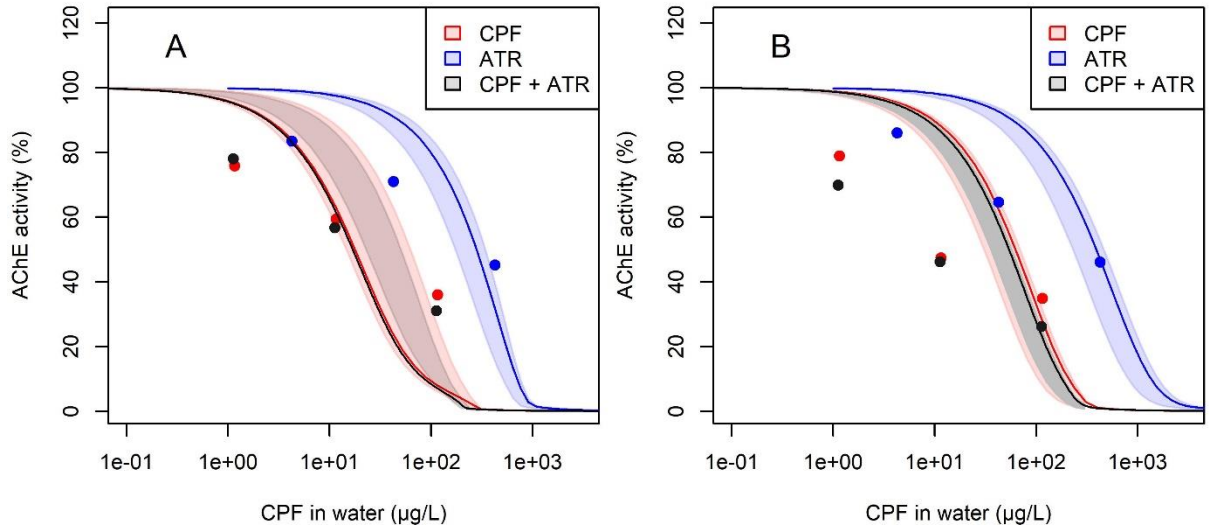

Figure S11: Predicted and observed AChE activity in muscle (A) and in brain (B) after 40 days continuous exposure in water. Observations are in carp, predictions are obtained with the fathead minnow PBTK-TD model

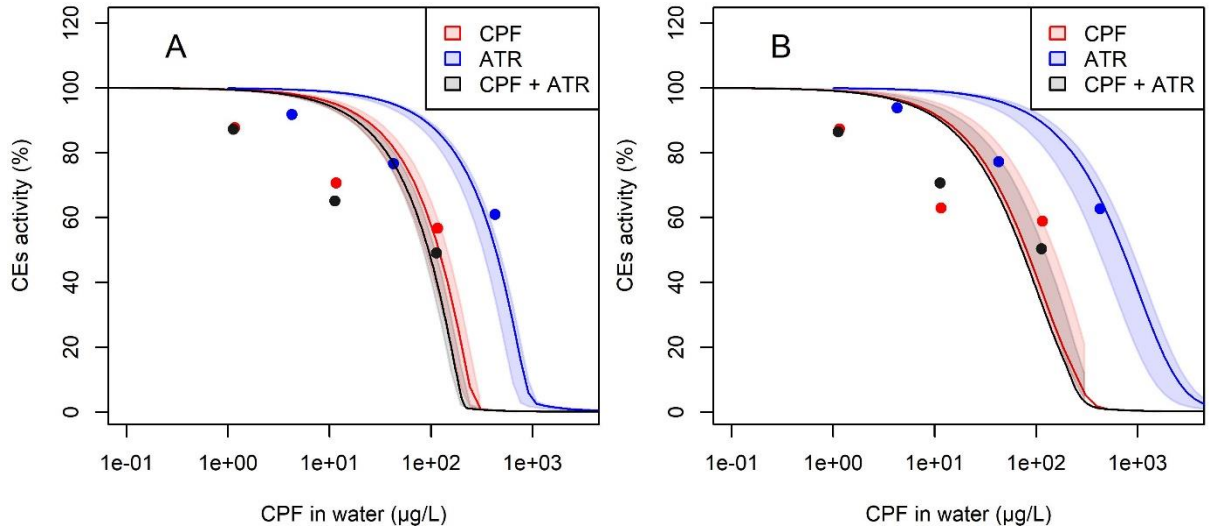

Figure S12: Predicted and observed CEs activity in muscle (A) and in brain (B) after 40 days continuous exposure in water. Observations are in carp, predictions are obtained with the fathead minnow PBTK-TD model

The dose-response relationships of the an equitoxic mixture of ATR an CPF (15 times more ATR than CPF) was predicted using the concentration addition model based on the dose-responses predicted with the PBTK-TD model (Figure S13).

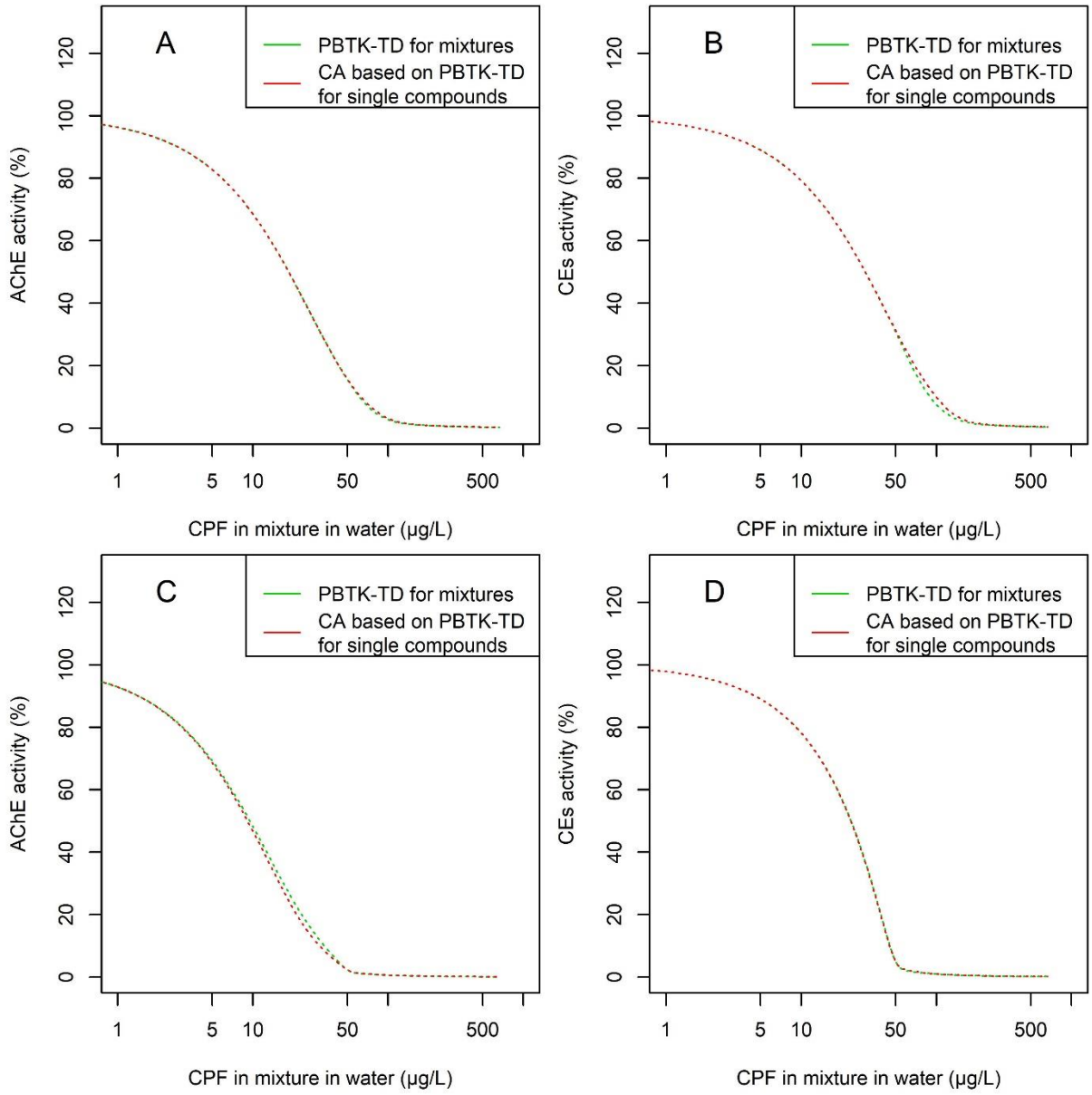

Figure S13: Predicted dose-responses obtained using the PBTK-TD model for mixtures, using and the concentration addition model based on the dose-responses predicted with the PBTK-TD model for single compounds, in brain (A, C) and muscle (B, D) for AChE (A, B) and CEs (C, D).

4.4. Comparison of internal concentrations at equal external exposure

Internal concentrations of CPF and CPF-oxon resulting from exposure to 11.3 µg/L CPF in water (which is the medium level in the mixture dose-response by Xing et al. (2010)) and ATR internal concentrations resulting from exposure to 11.3 µg/L ATR in water are reported in Table S10.

Table S10: Predicted internal concentrations of CPF, CPF-oxon, and ATR resulting from a continuous exposure to CPF or to ATR at 11.3µg/L in water.

	Internal concentration (µg/g)		
	Brain	Muscle	Whole body
Chlorpyrifos	1.48	0.501	1.22
Chlorpyrifos-oxon	0.0492	0.0169	0.0426
Atrazine	0.00605	0.000159	0.003

4.5. Comparison of binding to enzymes at equal internal concentrations

Enzyme activity was predicting by considering each enzyme independently and are not representative of the inhibition predicted in the tissues when both enzymes are modelled.

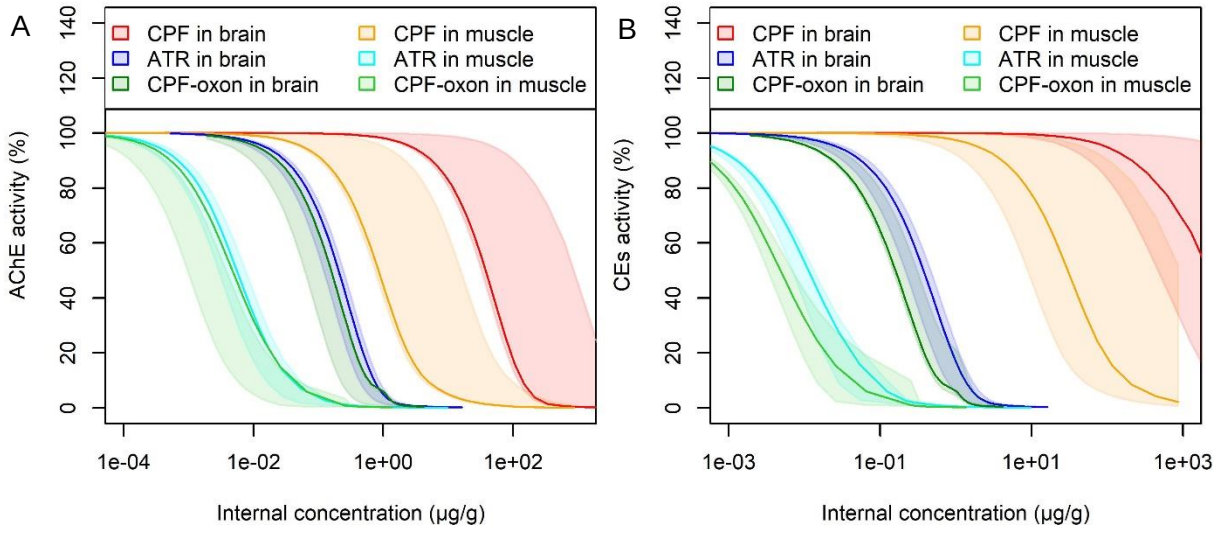

Figure S14: Predicted AChE (A) and CEs (B) activity resulting from exposure to CPF, CPF-oxon, and ATR, as a function of internal concentrations after 40 days of continuous exposure to ATR or CPF, in brain and in poorly perfused tissues (muscle) predicted with the best-fit estimates.

4.6. Effect of binding to AChE and CEs on internal levels of CPF, ATR, and CPF-oxon

Internal concentration levels of CPF, CPF-oxon, and ATR were estimated with the PBTK-TD model and without the TD part of the model. Levels in muscle were particularly impacted at low doses, until esterase inhibition was significantly inhibited (Figure S15).

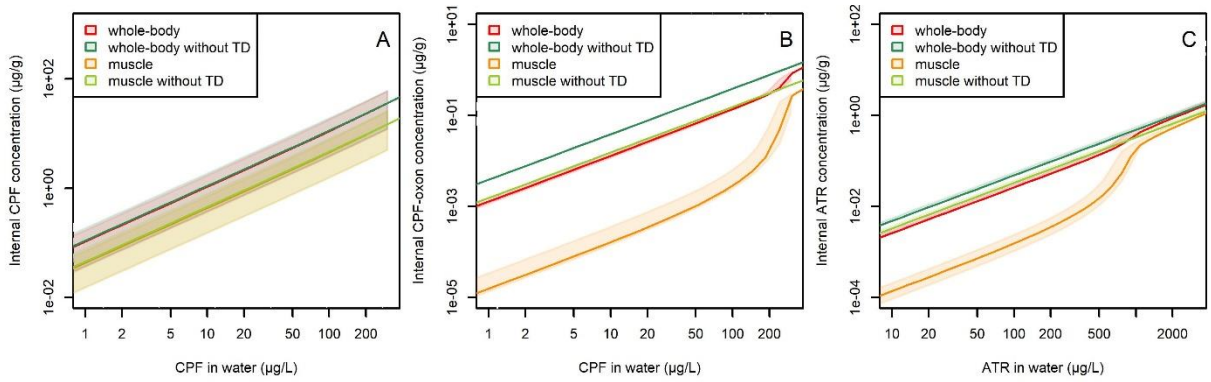

Figure S15: Predicted internal concentration levels of CPF (A) CPF-oxon (B), and ATR (C) that resulted from waterborne exposure to CPF or ATR, in muscle and in whole-body, with and without the TD submodel.

4.7. Effect of binding to CEs on AChE inhibition dose-response

The calibrated PBTK model was used to investigate the effect of binding to CEs on AChE inhibition resulting from exposure to a mixture of ATR and CPF (Figure S18). The slope of the dose-responses on a log-scale of concentrations was unchanged by the presence of CEs. Binding to enzymes is modelled in such a way that the presence of CEs decreases the amount of CPF by a factor (around 10 in muscle, and 2 in brain) that is independent of the exposure concentrations. The effect was particularly strong in the muscle due to large amount of CEs estimated in muscles.

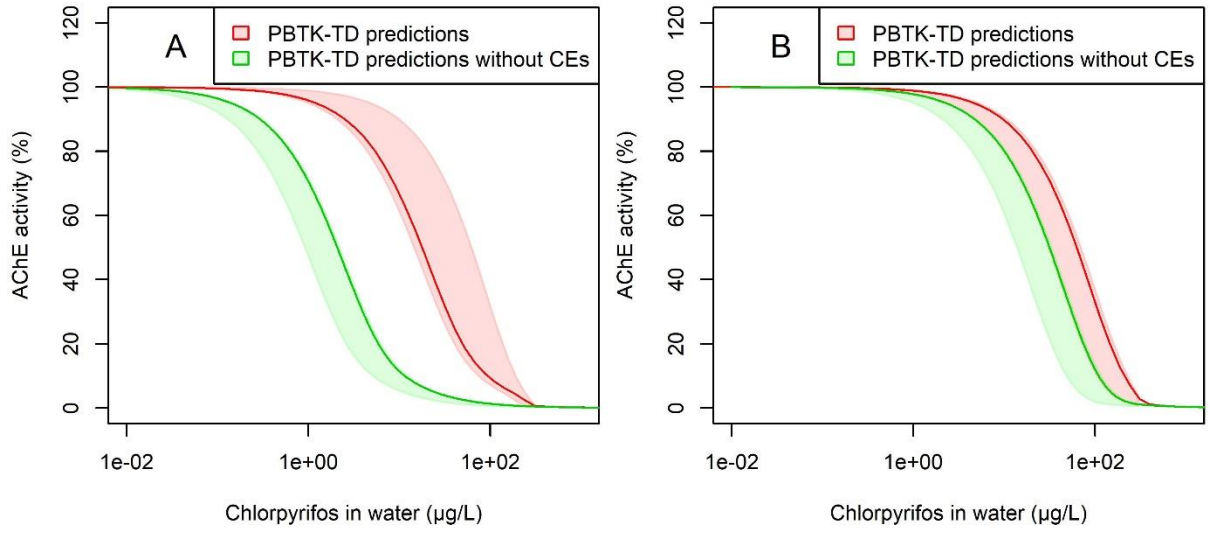

Figure S16: Predicted AChE inhibition in muscle (A), and in brain (B) resulting from continuous exposure to CPF for 40d, obtained with the PBTK-TD model (red), and with the PBTK-TD model without modelling CEs (green). The shaded areas represented the 95% prediction interval.

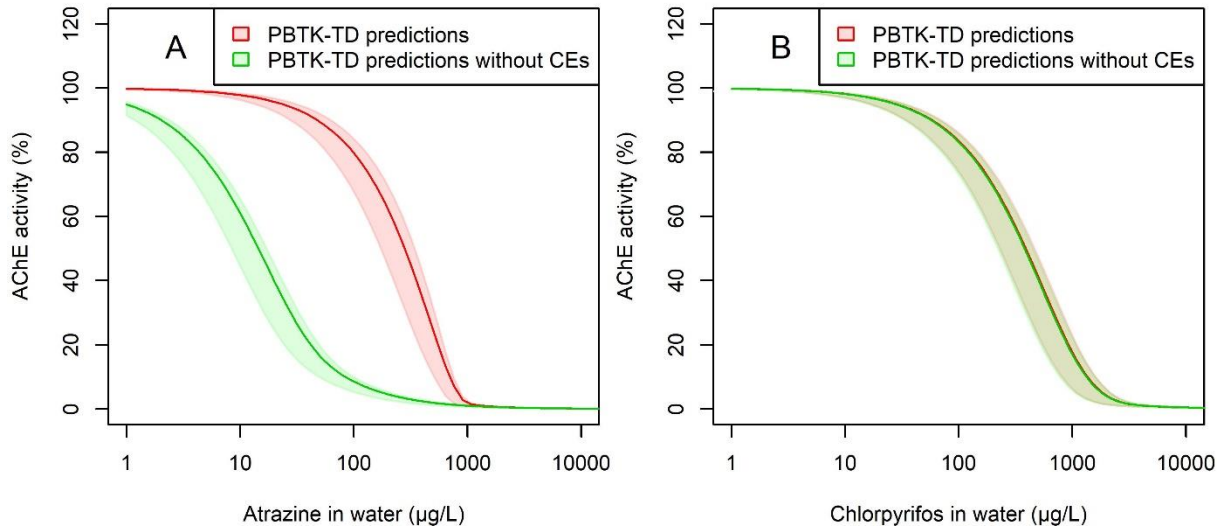

Figure S17: Predicted AChE inhibition in muscle (A), and in brain (B) resulting from continuous exposure to ATR for 40d, obtained with the PBTK-TD model (red), and with the PBTK-TD model without modelling CEs (green). The shaded areas represented the 95% prediction interval.

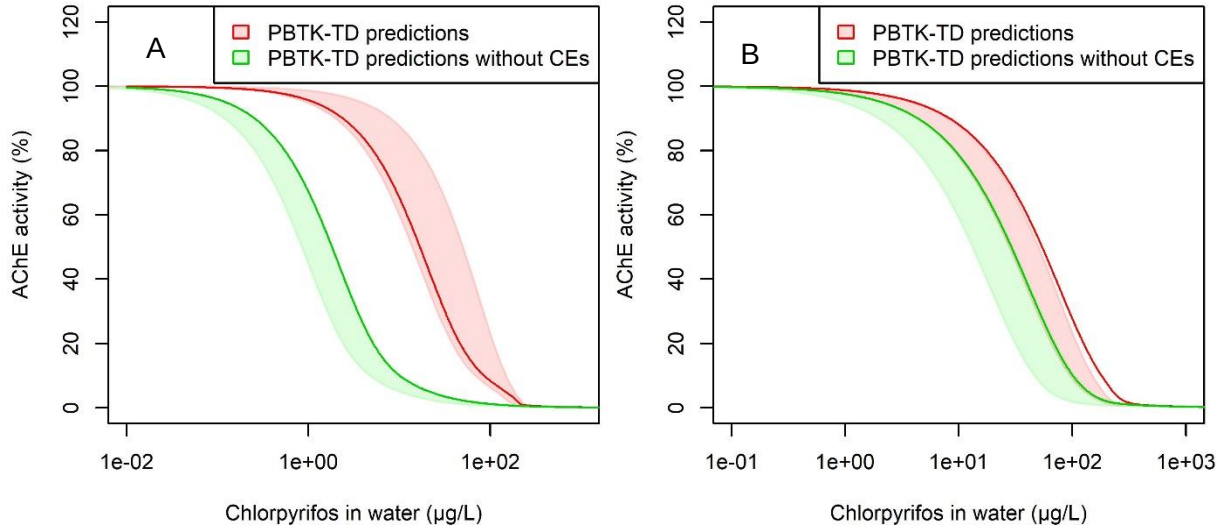

Figure S18: Predicted AChE inhibition in muscle (A), and in brain (B) resulting from continuous exposure to a mixture of ATR and CPF for 40d, obtained with the PBTK-TD model (red), and with the PBTK-TD model without modelling CEs (green). The shaded areas represented the 95% prediction interval.

5. References

1. Grech, A.; Tebby, C.; Brochot, C.; Bois, F. Y.; Bado-Nilles, A.; Dorne, J. L.; Quignot, N.; Beaudouin, R., Generic physiologically-based toxicokinetic modelling for fish: Integration of environmental factors and species variability. *Sci. Total Environ.* **2019,** *651*, 516-531.
2. Kooijman, B.; Kooijman, S., *Dynamic energy budget theory for metabolic organisation*. Cambridge university press: 2010.
3. Gunkel, G.; Streit, B., Mechanisms of bioaccumulation of a herbicide (atrazine, s-triazine) in a fresh-water mollusk (*Ancylus-fluviatilis Mull*) and a fish (*Coregonus-fera Jurine*). *Water Research* **1980,** *14*, (11), 1573-1584.
4. Barron, M. G.; Plakas, S. M.; Wilga, P. C.; Ball, T., Absorption, tissue distribution and metabolism of chlorpyrifos in channel catfish following waterborne exposure. *Environmental Toxicology and Chemistry* **1993,** *12*, (8), 1469-1476.
5. Gorge, G.; Nagel, R., Kinetics and metabolism of 14c-lindane and 14c-atrazine in early life stages of zebrafish (*Brachydanio-rerio*). *Chemosphere* **1990,** *21*, (9), 1125-1137.
6. Mehler, W. T.; Schuler, L. J.; Lydy, M. J., Examining the joint toxicity of chlorpyrifos and atrazine in the aquatic species: *Lepomis macrochirus*, *Pimephales promelas* and *Chironomus tentans*. *Environmental Pollution* **2008,** *152*, (1), 217-224.
7. Sandahl, J. F.; Jenkins, J. J., Pacific steelhead (Oncorhynchus mykiss) exposed to chlorpyrifos: Benchmark concentration estimates for acetylcholinesterase inhibition. *Environmental Toxicology and Chemistry* **2002,** *21*, (11), 2452-2458.
8. Wacksman, M. N.; Maul, J. D.; Lydy, M. J., Impact of atrazine on chlorpyrifos toxicity in four aquatic vertebrates. *Archives of Environmental Contamination and Toxicology* **2006,** *51*, (4), 681-689.
9. Wheelock, C. E.; Eder, K. J.; Werner, I.; Huang, H. Z.; Jones, P. D.; Brammell, B. F.; Elskus, A. A.; Hammock, B. D., Individual variability in esterase activity and CYP1A levels in Chinook salmon (Oncorhynchus tshawyacha) exposed to esfenvalerate and chlorpyrifos. *Aquatic Toxicology* **2005,** *74*, (2), 172-192.
10. Sturm, A.; Radau, T. S.; Hahn, T.; Schulz, R., Inhibition of rainbow trout acetylcholinesterase by aqueous and suspended particle-associated organophosphorous insecticides. *Chemosphere* **2007,** *68*, (4), 605-612.
11. Schmidel, A. J.; Assmann, K. L.; Werlang, C. C.; Bertoncello, K. T.; Francescon, F.; Rambo, C. L.; Beltrame, G. M.; Calegari, D.; Batista, C. B.; Blaser, R. E.; Roman Júnior, W. A.; Conterato, G. M. M.; Piato, A. L.; Zanatta, L.; Magro, J. D.; Rosemberg, D. B., Subchronic atrazine exposure changes defensive behaviour profile and disrupts brain acetylcholinesterase activity of zebrafish. *Neurotoxicology and Teratology* **2014,** *44*, 62-69.
12. Jarvinen, A. W.; Nordling, B. R.; Henry, M. E., Chronic toxicity of dursban (chlorpyrifos) to the fathead minnow (*Pimephales-promelas*) and the resultant acetylcholinesterase inhibition. *Ecotoxicology and Environmental Safety* **1983,** *7*, (4), 423-434.
13. Xing, H. J.; Wang, J. T.; Li, J. L.; Fan, Z. T.; Wang, M.; Xu, S. W., Effects of atrazine and chlorpyrifos on acetylcholinesterase and Carboxylesterase in brain and muscle of common carp. *Environ. Toxicol. Pharmacol.* **2010,** *30*, (1), 26-30.
14. Timchalk, C.; Nolan, R. J.; Mendrala, A. L.; Dittenber, D. A.; Brzak, K. A.; Mattsson, J. L., A Physiologically Based Pharmacokinetic and Pharmacodynamic (PBPK/PD) Model for the Organophosphate Insecticide Chlorpyrifos in Rats and Humans. *Toxicological Sciences* **2002,** *66*, (1), 34-53.
15. Maxwell, D. M., The specificity of carboxylesterase protection against the toxicity of organophosphorus compounds. *Toxicology and Applied Pharmacology* **1992,** *114*, (2), 306-312.
16. Abbas, R.; Hayton, W. L., A physiologically based pharmacokinetic and pharmacodynamic model for paraoxon in rainbow trout. *Toxicology and Applied Pharmacology* **1997,** *145*, (1), 192-201.

17. Johnson, J. A.; Wallace, K. B., Species-related differences in the inhibition of brain acetylcholinesterase by paraoxon and malaoxon. *Toxicology and Applied Pharmacology* **1987,** *88*, (2), 234-241.
18. Sandahl, J. F.; Baldwin, D. H.; Jenkins, J. J.; Scholz, N. L., Comparative thresholds for acetylcholinesterase inhibition and behavioral impairment in coho salmon exposed to chlorpyrifos. *Environmental Toxicology and Chemistry* **2005,** *24*, (1), 136-145.
19. Abbas, R. A physiologically based pharmacokinetic and pharmacodynamic model for paraoxon in rainbow trout. The Ohio State University, 1994.
20. Michalek, H.; Meneguz, A.; Bisso, G. M., Mechanisms of recovery of brain acetylcholinesterase in rats during chronic intoxication by isoflurophate. *Archives of toxicology. Supplement. = Archiv fur Toxikologie. Supplement* **1982,** *5*, 116-9.
21. Gearhart, J. M.; Jepson, G. W.; Clewell, H. J.; Andersen, M. E.; Conolly, R. B., Physiologically based pharmacokinetic and pharmacodynamic model for the inhibition of acetylcholinesterase by diisopropyfluorophosphate. *Toxicology and Applied Pharmacology* **1990,** *106*, (2), 295-310.
22. Traina, M. E.; Serpietri, L. A., CHANGES IN THE LEVELS AND FORMS OF RAT PLASMA CHOLINESTERASES DURING CHRONIC DIISOPROPYLPHOSPHOROFLUORIDATE INTOXICATION. *Biochemical Pharmacology* **1984,** *33*, (4), 645-653.
23. Timchalk, C.; Poet, T. S., Development of a physiologically based pharmacokinetic and pharmacodynamic model to determine dosimetry and cholinesterase inhibition for a binary mixture of chlorpyrifos and diazinon in the rat. *Neurotoxicology* **2008,** *29*, (3), 428-443.
24. Maxwell, D. M.; Lenz, D. E.; Groff, W. A.; Kaminskis, A.; Froehlich, H. L., The effects of blood flow and detoxification on in vivo cholinesterase inhibition by Soman in rats. *Toxicology and Applied Pharmacology* **1987,** *88*, (1), 66-76.
25. Maxwell, D. M.; Vlahacos, C. P.; Lenz, D. E., A PHARMACODYNAMIC MODEL FOR SOMAN IN THE RAT. *Toxicology Letters* **1988,** *43*, (1-3), 175-188.
26. Brown, R. P.; Delp, M. D.; Lindstedt, S. L.; Rhomberg, L. R.; Beliles, R. P., Physiological parameter values for physiologically based pharmacokinetic models. *Toxicology and Industrial Health* **1997,** *13*, (4), 407-484.
27. Bennett, M. K.; Erondu, N. E.; Kennedy, M. B., Purification and characterization of a calmodulin-dependent protein kinase that is highly concentrated in brain. *The Journal of biological chemistry* **1983,** *258*, (20), 12735-44.
28. Rodnick, K. J.; Holloszy, J. O.; Mondon, C. E.; James, D. E., Effects of exercise training on insulin-regulatable glucose-transporter protein levels in rat skeletal muscle. *Diabetes* **1990,** *39*, (11), 1425-9.
29. Schimke, R. T., Differential effects of fasting and protein-free diets on levels of urea cycle enzymes in rat liver. *The Journal of biological chemistry* **1962,** *237*, 1921-4.
30. Wallace, K. B.; Herzberg, U., Reactivation and aging of phosphorylated brain acetylcholinesterase from fish and rodents. *Toxicology and Applied Pharmacology* **1988,** *92*, (2), 307-314.
31. Yang, T. H.; Somero, G. N., Effects offeeding and food-deprivation on oxygen consumtion, muscle protein concentration and activities of energy-metabolism enzymes in muscle and brain of shallow-living (Scorpaena guttata) and deep-living (Sebastolobus alascanus) scorpaenid fishes. *Journal of Experimental Biology* **1993,** *181*, 213-232.
32. Peragon, J.; Barroso, J. B.; de la Higuera, M.; Lupianez, J. A., Relationship between growth and protein turnover rates and nucleic acids in the liver of rainbow trout (Oncorhynchus mykiss) during development. *Canadian Journal of Fisheries and Aquatic Sciences* **1998,** *55*, (3), 649-657.
33. Peragón, J.; Barroso, J. B.; García-Salguero, L.; de la Higuera, M.; Lupiáñez, J. A., Growth, protein-turnover rates and nucleic-acid concentrations in the white muscle of rainbow trout during development. *The international journal of biochemistry & cell biology* **2001,** *33*, (12), 1227-38.
34. R Core Team *R: A Language and Environment for Statistical Computing*, R Foundation for Statistical Computing: 2016.

35. Plummer, M.; Best, N.; Cowles, K.; Vines, K., CODA: Convergence Diagnosis and Output Analysis for MCMC. *R News* **2006,** *6*, (1), 7-11.
36. Gelman, A.; Rubin, D., Inference from iterative simulation using multiple sequences. *Statistical Science* **1992,** *7*, 457-511.
37. Saltelli, A.; Chan, K.; Scott, E. M., *Sensitivity Analysis*. John Wiley & Sons, Ltd ed.; New York, 2008.
38. Sobol, I. M.; Tarantola, S.; Gatelli, D.; Kucherenko, S. S.; Mauntz, W., Estimating the approximation errors when fixing unessential factors in global sensitivity analysis. *Reliability Engineering & System Safety* **2007,** *92*, 957-960.